Induced pluripotent stem cell derived monocytes and macrophages mimic human derived monocyte and macrophage phenotype and functionality and can be used model human inflammation and vascular dysfunction

Author: Emile van Vliet **Student number:** 5859441 **e-mail:** e.f.vanvliet@students.uu.nl
University: Utrecht University **Master programme:** Regenerative Medicine and Technology
Supervisor: Elise Kessler **e-mail:** e.l.kessler@umcutrecht.nl
First examiner: Saskia de Jager **Second examiner:** Alain van Mil

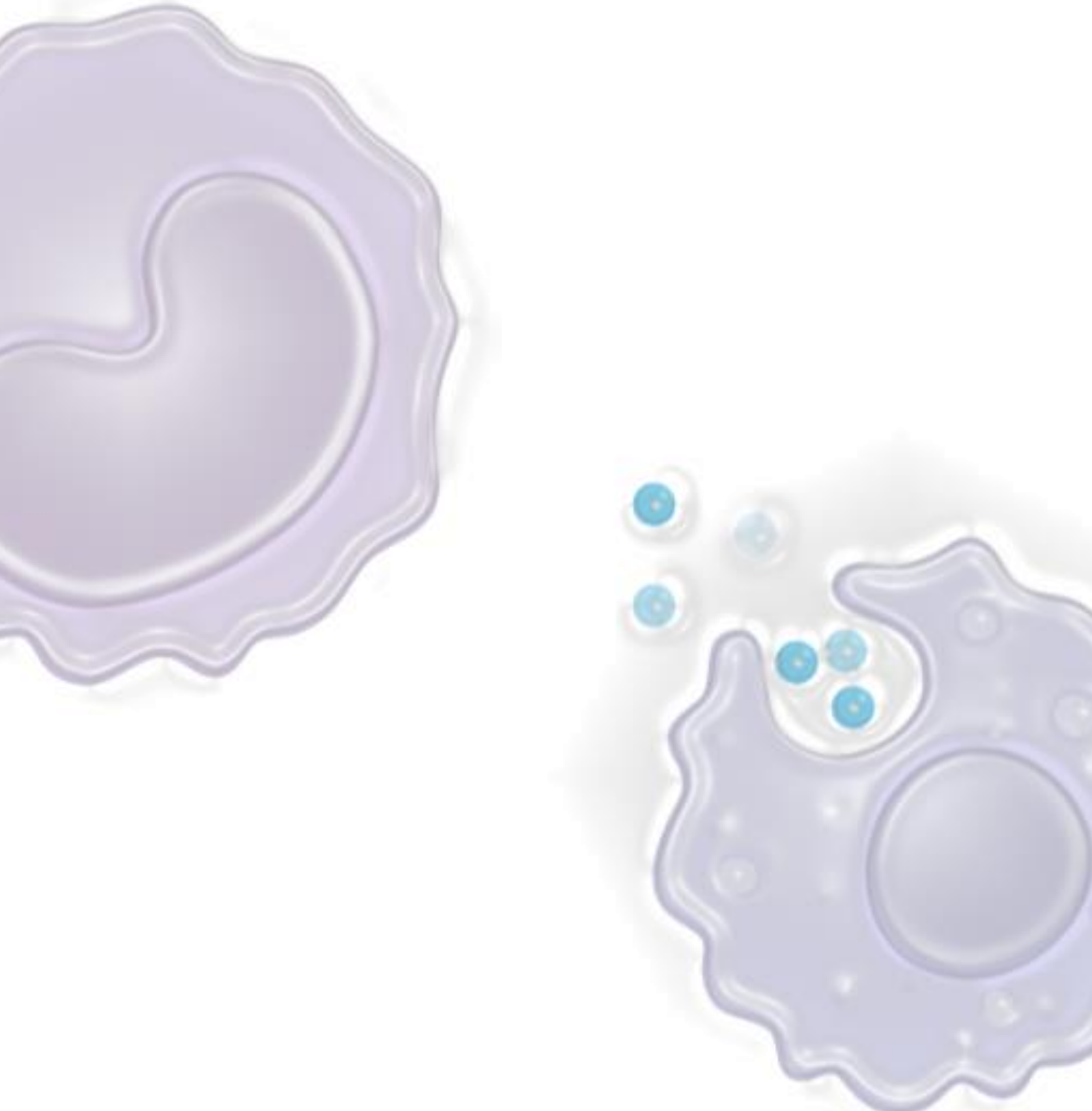

Abstract

Background

Monocytes and macrophages of the innate immune system play major roles in the onset and progression of cardiovascular diseases (CVDs). However, these cells are often not included in model systems due to difficulties in consistently isolating these cells out of peripheral blood mononuclear cells (PBMCs), warranting an alternative cell source. In this report, I investigated the use of human induced pluripotent stem cell (hiPSC) derived monocytes and macrophages to model human inflammation, comparing them to PBMC-derived monocytes and macrophages based on the following 8 pre-set definitions. Monocytes are round and granulated cells (1) that can be divided into 3 subsets based on CD14 and CD16 expression (2), should be able to interact with vasculature (3) and should be able to differentiate into macrophages (4). Macrophages are granulated cell types (5) that can be divided into 3 subsets based on CD163, CD64, CD80 and CD206 marker expression (6) and should functionally be able of phagocytosis (7) and cytokine secretion (8).

Materials and methods

To research the similarities between hiPSC-derived and PBMC-derived monocytes and macrophages, hiPSCs from three different cell lines were differentiated to monocytes. These monocytes were phenotypically analysed using microscopy and flow cytometry analysis on monocyte markers CD14, CD16, CCR2 and CX3CR1 marker expression, and functionally analysed by determining hiPSC-derived monocyte-EC interactions after activation with TNF-α under flow. the hiPSC-derived monocytes were polarised into M0, M1 and M2 macrophages and compared to PBMC-derived macropahges using flow cytometry analysis on macrophage markers CD163, CD64, CD80 and CD206.

Results

I demonstrated the successful differentiation of hiPSC-derived monocytes that could be divided into classical, non-classical and intermediate monocytes based on CD14 and CD16 expression, similar to PBMC-derived monocytes. These hiPSC-derived monocytes were functional and able to interact with endothelial cells under flow, which increased after activation with TNF-α. hiPSC-derived monocytes were successfully polarised towards M0, M1 and M2 macrophages that closely resembled PBMC-derived macrophages based on morphology and CD163, CD64, CD80 and CD206 marker expression.

Discussion

I illustrated succesfull hiPSC-derived monocyte generation which phenotypically and functionally resembled PBMC-derived monocytes and showed that these monocytes could be polarised into all three hiPSC-derived macrophage subsets that were phenotypically similar to PBMC-derived macrophages. These data suggest that hiPSC-derived monocytes and macrophages can be used to model human inflammation, however, additional macrophage functionality assays are required before I can confidenly confirm this hypothesis.

Layman's Summary

While immune cells play a big role in many heart diseases, it is difficult to mimic these immune cells and their function outside the human body. These problems appear because these immune cells are slightly different in every person, causing different results when we try to experiment with them. In this report, I researched if I could make these immune cells out of stem cells, and I compared the structure and function of these self-made immune cells to immune cells isolated from the human blood, to see if these cells can be used to model heart disease.

To research the similarities between the self-made immune cells and the cells isolated from the human blood, I made immune cells from three different donors. These immune cells were compared to blood-isolated immune cells based on looks/structure and expression of different cell surface markers that are specific for these immune cells. I also compared the functionality of my self-made immune cells to immune cells isolated from human blood by mimicking flow though a human vein, and looking at the interactions of the self-made immune cells to the cells of the vein.

After performing the experiments, I saw that my self-made immune cells looked similar to immune cells isolated from the human body through the microscope, and the markers present on the cell surface. Additionally, the interactions of the self-made immune cells with the cells of the vein were similar to the blood-derived immune cells as well, confirming that the cells I made are functional.

Therefore, I can conclude that the self-made immune cells are similar to immune cells isolated from the human blood, both structurally and functionally. This suggests that the self-made immune cells can be used to mimic heart disease outside of the human body. However, before these cells can actually be used to mimic human heart disease, more experiments on the functionality of the self-made immune cells is required.

1. Introduction

1.1 Monocytes and macrophages in cardiovascular disease

Cardiovascular diseases (CVDs) are the leading cause of death globally, with limited treatment options available until this day (Virani, Alonso et al. 2020, Leong, Joseph et al. 2017). In an attempt to study the pathophysiology of these CVDs and to develop novel treatment options, recent research has led to the creation of several 2D and 3D *in vitro* models, including cell types like cardiomyocytes (CMs), endothelial cells (ECs) an fibroblasts (Nugraha, Buono et al. 2019). However, while the majority of CVDs are inflammation driven, where sustained activation of monocytes and macrophages from the innate immune system induces cardiac/vascular damage and remodelling, these innate immune cells are severely underrepresented or absent in *in vitro* models designed to study CVDs (Jaén, Val-Blasco et al. 2020, Lippi, Stadiotti et al. 2020). Monocytes and macrophages are often not included in disease models due to limited knowledge on their origin and function of these cell types, as well as limitations in the cell sources that are currently used to acquire these monocytes and macrophages (Lippi, Stadiotti et al. 2020). The absence of these innate immune cells result in inaccurate modelling of CVD pathophysiology *in vitro,* greatly hindering our understanding of disease mechanisms and resulting in translational problems when trying to bring novel treatments to the clinic (Nugraha, Buono et al. 2019). Recent research has illustrated that human induced pluripotent stem cells (hiPSCs) can be differentiated towards monocytes and then polarised towards macrophages by mimicking the development of tissue-derived monocytes and macrophages. In addition it has been shown that the produced hiPSC-derived monocytes and macrophages are similar to their blood-derived counterparts (Buchrieser, James et al. 2017, Cao, Yakala et al. 2019, Karlsson, Cowley et al. 2008). I therefore hypothesize that hiPSC-derived monocytes and macrophages are phenotypically and functionally similar to blood-derived monocytes and macrophages, and can be used to model human inflammation in CVDs and vascular dysfunction *in vitro.* However, before these hiPSC-derived monocytes and macrophages can be included in CVD models, additional knowledge on different monocyte and macrophage subsets that are created is required, as well as how these hiPSC-derived monocytes and macrophages functionally compare to blood-derived monocytes and macrophages. In this study, I investigated if hiPSC-derived monocytes and macrophages phenotypically and functionally resembled blood-derived monocytes and macrophages according to the monocyte and macrophage definitions provided in section 1.2 and Fig.1, to determine if these hiPSC-derived monocytes and macrophages can be used to model human inflammation and vascular dysfunction *in vitro*.

1.2 monocyte and macrophage definitions

Monocytes and macrophages are round, granulated cells of the innate immune system (Fig. 1 definition 1). that can be found both in the systemic circulation and in many tissues of the body like the heart, the skin, and the lungs (Monkley, Krishnaswamy et al. 2020). Monocytes and macrophages play vital roles in numerous processes throughout life including tissue homeostasis and repair, initiation and mediation of immune responses, clearance of pathogens, but also in the pathophysiology of many different immune related- and nonimmune related diseases like infections, cancer, and CVDs (Monkley et al. e0243807; Wolf et al. 1642). Whilst the different subtypes of monocyte and macrophage have been thoroughly researched and classified in mice (Lichanska, Browne et al. 1999, Gordon, Taylor 2005), human monocyte and macrophage classification remains poorly understood (Gordon, Taylor 2005, Karlsson, Cowley et al. 2008).

However, there are currently three known human monocyte subsets that can be distinguished based on their cluster of differentiation 14 (CD14) and cluster of differentiation 16 (CD16) expression and function: the $CD14^{++}$ $CD16^{-}$classical monocytes, the $CD14^{+}$ $CD16^{++}$ non-classical monocytes and the

$CD14^{++}$ $CD16^{+}$ intermediate monocytes (Fig. 1 definition 2) (Kapellos, Bonaguro et al. 2019). The classical monocyte's main function is migration towards site of inflammation through adhesion and interaction with vasculature (Fig. 1 definition 3) and facilitation of the anti-microbial response through secretion of pro-inflammatory cytokines like interleukin 4 (IL-4) and interleukin 10 (IL-10) (Kratofil, Kubes et al. 2017, Kapellos, Bonaguro et al. 2019, Williams, Huang et al. 2019). At the site of inflammation, the classical monocytes polarise towards pro-inflammatory "killer" M1 macrophages (Fig. 1 definition 4) which are round granulated cell types that usually co-localise closely together (Fig. 1 definition 5) and can be recognised by cluster of differentiation 163 (CD163), cluster of differentiation 64 (CD64) and cluster of differentiation 80 (CD80) marker expression (Fig. 1 definition 6). The main function of the M1 macrophage is phagocytosis and secretion of pro-inflammatory cytokines like tumor necroses factor-α (TNF-α), interleukin 1 beta (IL-1β) and interleukin 6 (IL-6) (Fig. 1 definition 7 and 8 (Yao, Xu et al. 2019). While the more mature non-classical monocytes are also able to secrete pro-inflammatory cytokines like TNF-α and interleukin 12 (IL-12), transmigrate and mediate the anti-microbial response, these monocytes polarise towards the anti-inflammatory "builder" M2 macrophages (Fig. 1 definition 4), which are stretched granulated cell types (Fig. 1 definition 5) that can be recognised by CD163 and cluster of differentiation 206 (CD206) marker expression (Fig. 1 definition 6 (Kapellos, Bonaguro et al. 2019). M2 macrophages mainly function in prevention of infections, phagocytosis (Fig. 1 definition 7) angiogenesis, immunomodulation and tissue repair through secretion of anti-inflammatory cytokines like IL-10 and growth factors like transforming growth factor beta (TGF-β) (Fig. 1 definition 7) (Kapellos, Bonaguro et al. 2019, Mantovani, Sica et al. 2004, Yao, Xu et al. 2019, Parisi, Gini et al. 2018). The intermediate monocytes, which show similarities to both classical and non-classical monocytes, mainly function in antigen presentation, but are also able of pro-inflammatory cytokine secretion (Kapellos, Bonaguro et al. 2019). These monocytes can polarise into either M1 or M2 macrophages and are able to influence inflammation based on the cytokines they encounter (Parisi, Gini et al. 2018, Wong, Tai et al. 2011). The full definitions of all known monocyte and macrophage subsets and their main functions are summarised in Fig. 1.

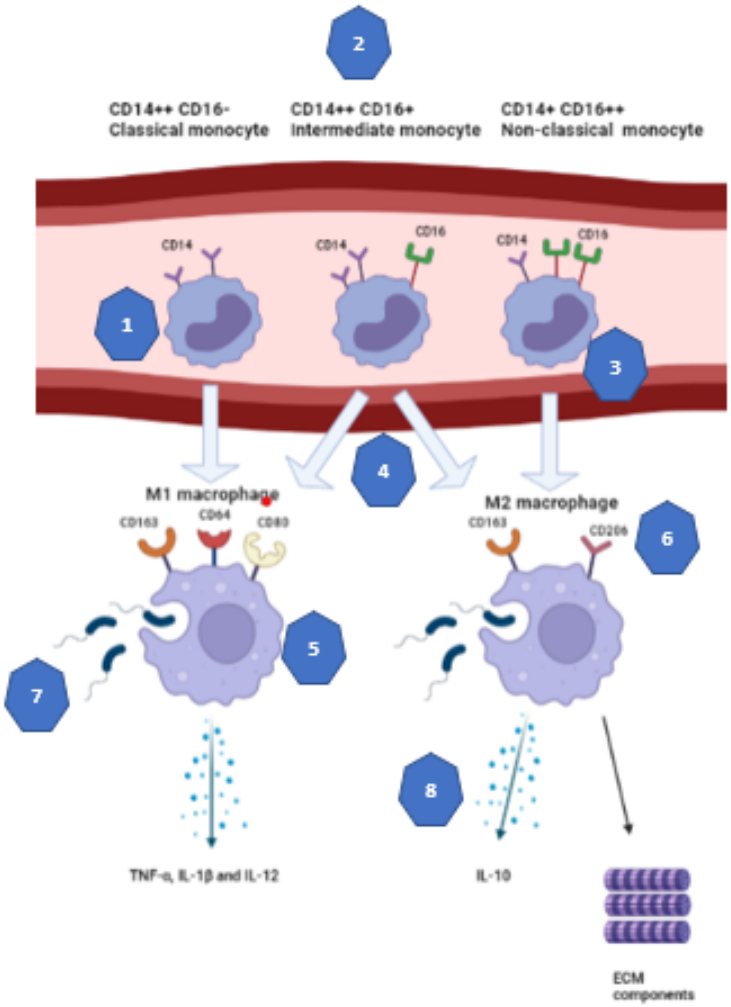

Figure 1. Monocyte and macrophage definitions. *Monocytes are round granulated cells (1) that can be divided into CD14++CD16- classical monocytes, CD14++CD16+ intermediate monocytes and CD14+CD16++ non-classical monocytes (2). These monocytes should be able to interact with- and transmigrate vasculature (3), after which they should be able to polarise into a phagocytotic cell type (4). Classical monocytes polarise into pro-inflammatory CD163+CD64+CD80+ M1 macrophages (6) which are round granulated cell types that usually cluster close together (5) and mainly function in pathogen clearance (7) and pro-inflammatory cytokine secretion like TNF-α and IL-12 (8). Non-classical monocytes polarise into anti-inflammatory CD163+CD206+ M2 macrophages which are stretched granulated cell types (6) and which function in pathogen clearance (7), secretion of anti-inflammatory cytokines like IL-10 (8), stimulation of angiogenesis and tissue repair through stimulation of ECM production and deposition. The intermediate monocytes are able to polarise into either M1 or M2 macrophages based on the type of cytokines that they encounter.*

1.3 human peripheral blood mononuclear cells in inflammation modelling

Current human monocyte and macrophage studies are usually performed on monocytes isolated from peripheral blood mononuclear cells (PBMCs), however the use of PBMC-derived monocytes has several downsides and leads to difficulties in consistency and translatability of research (Monkley, Krishnaswamy et al. 2020). First and foremost, it is difficult to obtain enough donor blood for cell batches that are large enough to facilitate controlled research, especially for donor blood of patients with rare diseases (Cao, Yakala et al. 2019). Another problem is the batch-to-batch variety of the monocytes and macrophages. This monocyte and macrophage variety does not only consist between different blood donors due to different genetics, but also between batches of the same donor based on the physiological state of the donor and antigens that these cells encountered at different donations (van Wilgenburg, Browne et al. 2013). These in-donor differences, which can result in the isolation of different subsets of monocytes with different levels of activation, requires the use of many different donors at once to guarantee that observations made are representative of (patho)physiological conditions, increasing the patient burden (van Wilgenburg, Browne et al. 2013).

In addition to these difficulties in consistency and translatability when using PBMC-derived monocytes, recent research has indicated a difference in developmental ontogeny between tissue resident macrophages and bone marrow-derived PBMC-derived macrophages. While PBMC-derived macrophages decent from hematopoietic stem cells (HSCs) from the aorta-gonad-mesonephros region (AGM) in a homeobox A cluster (HOXA) dependent manner during wave 3 of the

hematopoietic development (Dou, Calvanese et al. 2016, Cao, Yakala et al. 2019), it is now believed that tissue resident macrophages are derived from the primitive erythron-myeloid progenitors (EMPs) produced in the yolk-sac in a MYB Proto-Oncogene (MYB) independent manner during wave 1 and 2 of hematopoietic development (Fig. 2) (Buchrieser, James et al. 2017, Cao, Yakala et al. 2019). The PBMC-derived monocyte and macrophage populations are sustained by myeloid precursor cells located in the bone marrow for the remainder of adult life. These precursor cells give rise to pro-inflammatory immature $CD14^{++}$ $CD16^{-}$ classical monocytes, which are the only monocyte subset found within the bone marrow, and are immobilised and anchored within the bone marrow through CCR2-CXCR4 complexes, marking their immaturity (Kapellos, Bonaguro et al. 2019, Al-Rashoudi, Moir et al. 2019, Patel, Zhang et al. 2017). After partial CCR2 internalisation in response to inflammatory stimuli, classical monocytes are released and migrate towards the circulation, where surviving monocytes steadily mature and give rise to $CD14^{++}$ $CD16^{+}$ intermediate monocytes and eventually the mature anti-inflammatory CX3C chemokine receptor 1 $(CX3CR1)^{+}$ $CD14^{+}$ $CD16^{++}$ non-classical monocytes (Kapellos, Bonaguro et al. 2019, Al-Rashoudi, Moir et al. 2019, Patel, Zhang et al. 2017). On the other hand, tissue-resident monocyte and macrophage populations sustain themselves independently of circulating monocytes by self-renewal after tissue engraftment in a MYB-independent manner (Fig. 2) (Ginhoux, Jung 2014). This observation makes it impossible to study tissue-resident macrophages and their impact on inflammation and pathophysiology using PBMC-derived monocytes and macrophages, as these cell types are not present within the donor blood (Lee, Kozaki et al. 2018). The above-mentioned problems warrant a novel monocyte and macrophage model system, which represents both PBMC-derived and tissue-resident monocytes and macrophages that can be consistently harvested in large quantities.

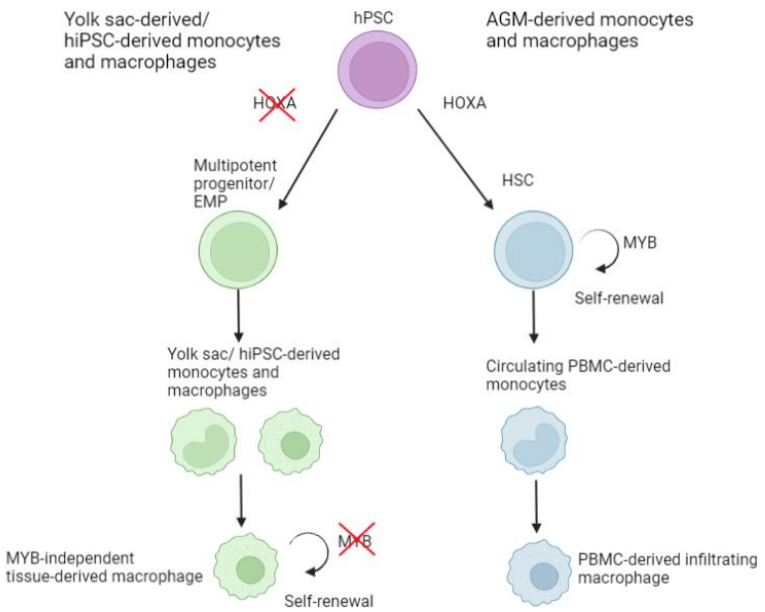

Figure 2. Development and origin of hiPSC-derived, tissue derived and PBMC-derived monocytes and macrophages. *During the development of yolk sac-derived and hiPSC-derived monocytes and macrophages, hPSCs differentiate into multipotent progenitors and EMPs in a HOXA independent manner, after which tissue-resident monocytes and macrophages are formed. These tissue-resident macrophages self-renew in a MYB Proto-Oncogene (MYB) independent manner. On the other hand, PBMC-derived monocytes and macrophages are created by hPSC differentiation into HSCs in a HOXA dependent manner. These HSCs are able to differentiate into circulating monocytes and macrophages and replenish the circulating monocyte and infiltrating macrophage populations through MYB-dependent self-renewal. This figure is adapted from (Buchrieser, James et al. 2017*

1.4 hiPSC-derived monocytes and macrophages as cell source for inflammation modelling

Recent studies have indicated the possibility to produce monocytes out of hiPSCs, which can be further polarised into macrophages as an alternative cell source to PBMC-derived monocytes and macrophages (Buchrieser, James et al. 2017, Happle, Lachmann et al. 2018, Karlsson, Cowley et al. 2008, Lang, Cheng et al. 2018). The advantage of these hiPSC-derived monocytes and macrophages are that they are of human origin and are therefore translatable into the clinic (Yanagimachi, Niwa et al. 2013, Monkley, Krishnaswamy et al. 2020).

Additionally, these hiPSC-derived monocytes and macrophages can be genetically manipulated to model certain disease phenotypes or can be derived in a patient specific manner to fully mimic disease genetics (Monkley, Krishnaswamy et al. 2020). Practical advantages of these hiPSC-derived monocytes and macrophages are that they are an indefinite cell source and do not display the batch-to-batch differences of PBMC isolated monocytes and macrophages, due to their genetic stability and consistent activation state (Monkley, Krishnaswamy et al. 2020). hiPSCs-derived monocytes are made by hiPSC differentiation into early hematopoietic progenitor cells, which in turn can give rise to hiPSC-derived monocytes and macrophages through MYB and HOXA independent myeloid differentiation, similar to yolk sac-derived EMPs found in mice (Fig. 2) (Cao, Yakala et al. 2019, Choi, Vodyanik et al. 2009, Dou, Calvanese et al. 2016, Buchrieser, James et al. 2017). As mentioned earlier, tissue resident monocytes and macrophages are derived from these yolk sac-derived EMPs (Cao, Yakala et al. 2019), suggesting a reliable cell source for the study of tissue-derived monocytes and macrophages *in vitro*. Buchrieser *et.al* demonstrated the successful hiPSC to monocyte and macrophage differentiation and elucidated their developmental ontogeny using an iPSC CRISPR-Cas9 knock-out system. They also illustrated that these monocytes and macrophages were morphologically similar to PBMC-derived monocytes and macrophages and started functional characterisation of these monocytes and macrophages. However, a more in-depth monocyte and macrophage characterisation on both phenotype and function (as described in Fig. 1) is required to confidently state that hiPSC-derived monocytes and macrophages resemble their human counterparts and can reliably be used as a model system for human blood and tissue-derived monocytes and macrophages.

Here, I illustrated the successful differentiation of three hiPSC lines (NP0 143-18, NP0 115-4H and NP0 144-41, characteristics of which are shown in Table 1) into monocytes according to the Buchrieser *et al*. protocol (Buchrieser, James et al. 2017). The harvested monocytes were characterised into classical, non-classical and intermediate monocytes based on CD14 and CD16 expression, after which their maturity and inflammatory potential was determined using CCR2 and CX3CR1 flow cytometry gating. These monocytes were then polarised towards M0, M1 and M2 macrophages and analysed on morphology compared to PBMC-derived monocytes. Additional hiPSC-monocyte functionality was then researched to determine monocyte-EC interactions under flow to mimic vascular dysfunction.

2. Materials and methods

2.1 Cell culture

hiPSCs from three healthy donors were used for the hiPSC to monocyte differentiation. The hiPSC-ECs used for the monocyte adherence under flow experiments were derived from these same three healthy donors. An overview of the characteristics of all three hiPSC donors is shown in Table 1.

Table 1. hiPSC donor overview showing donor number, sex, age, ethnicity and method of transfection

Donor	Sex	Age	Ethnicity	Method of transfection
NP0 143-18	Female	22	Caucasian	Sendai Virus
NP0 115-4H	Female	36	Chinese	Sendai Virus
NP0 144-41	Male	31	Caucasian	Sendai Virus

<u>hiPSC cell culture</u>

hiPSCs from all three donors were plated out on Matrigel (1.2 mg/ml Matrigel phenol red free growth factor reduced (Corning 356231, USA; in DMEM/F-12 (1:1) + GlutaMAX; Gibco 31331-028, UK) coated 6-wells plates (Corning 3506) in 2 mL Essential 8 (E8) culture medium (Gibco A15171-01, USA) containing 10 µM Rock inhibitor (Y-27632; BD Biosciences 562822, USA). hiPSCs received a daily E8 culture medium refresh and were passaged at 80% confluency by washing with Ca^{+} and Mg^{2+} free phosphate-buffered saline (PBS; pH 7.4 (1x; Gibco 10010-015)) after which hiPSCs were incubated with 0.5 mM Ethylenediamine tetraacetic acid (EDTA) (Invitrogen 15575-038, USA) for 3 min at 37 °C and detached by flushing with E8 medium. The flushed cells were transferred to new Matrigel coated 6-wells plates in a 1:7 to 1:20 ratio depending on the desired cell concentration.

<u>hiPSC endothelial cell culture</u>

hiPSC-ECs from all 3 donors were plated out on fibronectin (Sigma-Aldrich F1141, USA; diluted 1:50 in PBS) coated T25 culture flasks (Greiner bio-one Cellstar 690175, Germany) in iPSC-EC complete medium: endothelial cell basal medium 2- (Lonza CC-3156, Belgium) supplemented with 1% penicillin-streptomycin (Pen/Strep; Gibco 15140-122), 10% heat inactivated fetal bovine serum (FBS) (Corning 35-079-CV) and 1% GlutaMAX (2 mM, 100x; Gibco 35050-038). hiPSC-ECs received a complete culture medium refresh every other day and were passaged at 100% confluency by washing with Ca^{+} and Mg^{2+} free PBS after which hiPSC-ECs were incubated with Accutase (Innovative Cell Technologies AT-104, USA; diluted 1:2 in 500 mL distilled H_2O) for 3 min at 37 °C. Detached cells were centrifuged for 5 min at 350 xG, resuspended in iPSC-EC complete medium and transferred to a new T25 or T75 flask.

2.2 hiPSC to monocyte differentiation

During the hiPSC to monocyte differentiation, hiPSCs were differentiated towards primitive mesoderm, after which they differentiate along the myeloid lineage from hematopoietic progenitor cells to monocytes and macrophages. During this differentiation, hiPSCs were first clustered together to form embryonic bodies (EBs), which were matured, transferred to a gelatine coated 6-wells plate, and co-cultured with human macrophage colony-stimulating factor (hM-CSF) Peprotech AF-300-25; 100ng/mL) and human interleukin-3 (hIL-3) (Peprotech 200-03; 25ng/mL) to produce monocytes and macrophages, which could be harvested weekly. The different culture media used and the factors with which they were supplemented can be found in Table 2.

Table 2. Culture media used during the hiPSC to monocyte differentiation

EB medium: Used for generation of EBs and EB culture medium refresh on day 1 and day 2 of the hiPSC to monocyte differentiation.	E8 medium supplemented with: Human bone morphogenic protein 4 (hBMP4) (Peprotech 120-05, USA) (50 ng/mL) Human stem cell factor (hSCF) (Peprotech 300-07) (20 ng/mL) Human vascular endothelial growth factor (hVEGF) (Peprotech AF-100-20) (50 ng/mL) Rock Inhibitor (10 µM)
MM Differentiation medium: Used for EB transfer to gelatine coated 6-wells plates and every culture medium refresh afterwards.	X-VIVO Basal Medium 15 (Lonza BE02-060R) supplemented with: 1% Pen/Strep 1% GlutaMAX (2 mM, 100x) 0.1% ß-MercaptoEthanol (1000x, 55mM; Gibco 31350-010) hM-CSF (100 ng/mL) hIL-3 (25 ng/mL)
Macrophage Differentiation Medium: Used in the first week of monocyte to macrophage polarisation.	X-VIVO Basal Medium 15 supplemented with: 1% Pen/Strep 1% GlutaMAX (2 mM, 100x) 0.1% ß-MercaptoEthanol (1000x, 55mM) hM-CSF (100ng/ml)

Embryonic body generation (day 0)

EBs were generated by washing 2 wells of hiPSCs (80% confluency) with Ca^{+} and Mg^{2+} free PBS, after which the hiPSCs were detached by incubating 0.5 mL TrypLE Express (Gibco 12604013) for 3 min at 37 °C. hiPSCs were counted, centrifuged at 350 xG for 3 min and resuspended to 1.25 x 10^5 cells/mL in EB medium (Table 2). hiPSCs were plated out by transferring 100 µL cell suspension (1.25 x 10^4 hiPSCs) to 48 wells of a 96 wells ultra-low attachment plate (Corning 7007) and centrifuged for 3 min at 100 xG to form EBs, which were carefully stored at 37 °C. The EBs were matured for the next 4 days of the differentiation protocol.

Embryonic body medium refresh (day 1 and 2)

The next 2 days, EBs received an EB culture medium refresh by carefully aspirating 50 µL of culture medium after which 50 µL of fresh EB medium was added to the wells. EBs maturation was monitored by checking EB size, structure and EB core density after each culture medium refresh (Fig. 3A column 1).

Embryonic body transfer to gelatine coated 6-wells plates (day 4)

On day 4 of the hiPSC to monocyte differentiation, the EBs were transferred to a 0.2% gelatine (gelatine from porcine skin; Sigma-Aldrich 9000-70-8; 5 gram in 500 mL milli-Q = 1% stock solution, stock diluted to 0.2% in Ca^{+} and Mg^{2+} free PBS) coated 6-wells plate. 8 EBs were transferred per well of the gelatine coated 6-wells plate. The EB medium was then carefully removed from the plate without aspirating any EBs, after which each well received 2 mL of MM differentiation medium (Table 2). The EBs were carefully spread over the surface of the well and stored at 37 °C and 5% CO_2 in the incubator. The 6-wells plate and the incubator were not touched for the next 6 days.

Outgrowth medium refresh (day 10)

On day 10 of the hiPSC to monocyte differentiation protocol, all wells in the 6-wells plates carefully received 1 mL of MM differentiation medium (Table 2) without aspirating any old culture medium.

hiPSC-derived monocyte harvest (Once every 5-7 days)

Once every week for the next 5 weeks, the hiPSC derived monocytes were harvested by carefully aspirating two thirds of the MM differentiation medium, after which all wells received 2 mL of fresh MM diff medium. Attached monocytes were carefully flushed from the outgrowths by pipetting aspirated medium over these complexes in a dropwise manner.

2.3 PBMC and monocyte isolation from whole blood

As a control to hiPSC monocytes, mini donor dienst (MDD; blood donated at- and collected from the university medical centre (UMC) Utrecht after informed consent; code: F1P50) monocytes were isolated from PBMCs originating from the whole blood of healthy donors. PBMCs were isolated by Ficoll-paque plus (GE healthcare 17-1440-03, The Netherlands) density gradient centrifugation. Monocytes were isolated from these PBMCs using the STEMCELL technologies EasySep human monocyte enrichment kit without CD16 depletion (STEMCELL technologies 19058, Canada). The PBMCs were treated with deoxyribonuclease (DNAse; Stemcell 07900) for 15 min at RT, after which the cells were strained and transferred to a 5 mL polystyrene round-bottom tube (Corning 352058, Mexico), and the human monocyte enrichment cocktail (STEMCELL 19058C.2) was incubated for 10 min at 4 °C. After incubation, the EasySep D magnetic particles for human monocytes (STEMCELL 19550) were added to the cells and incubated for 5 min at 4 °C, after which the cells were placed in the EasyEight EasySep magnet (STEMCELL 18103, USA) for 2.5 min. Monocytes in suspension were then plated out for macrophage polarisation or stained for flow cytometry analysis.

2.4 Monocyte to macrophage polarisation

Freshly harvested hiPSC monocytes and freshly isolated PBMC-derived monocytes were resuspended in a density of 3.0 x 10^5 cells/mL in their corresponding culture media as mentioned in Table 3 and plated out in 24-wells plates (Corning 3524).

Table 3. Culture media used during the monocyte to macrophage polarisation

RMPI complete medium: Culture medium used during the monocyte to macrophage polarisation of PBMC-derived monocytes.	RMPI 1640 (1x) [+] L-Glutamine (Gibco 21875-034) medium supplemented with: 1% Pen/Strep 10% heat inactivated FBS
X-VIVO basal complete medium: Culture medium used during the monocyte to macrophage polarisation of hiPSC-derived monocytes	X-VIVO Basal Medium 15 supplemented with: 1% Pen/Strep 10% heat inactivated FBS 1% GlutaMAX (2 mM, 100x) 0.1% ß-MercaptoEthanol (1000x, 55mM)

The monocytes were polarised towards M0 macrophages by optimized stimulation conditions (100 ng/mL hM-CSF for hiPSC monocytes and 50 ng/mL hM-CSF for PBMC-derived monocytes), with a culture medium refresh containing hM-CSF once every 2 days. After 6 days, the M0 macrophages were polarised towards either M1 or M2 macrophages by culturing them with the following factors for 4 days (culture medium refresh supplemented with stimuli after 2 days):

- M0: RMPI1640 complete or X-VIVO basal complete.

- M1: RMPI 1640 or X-VIVO basal complete containing 10 ng/mL lipopolysaccharide (LPS) (Peprotech)
- 297-473-0) and 50 ng/mL human interferon gamma (hIFN-γ) (Peprotech P01579.1).
- M2: RMPI 1640 or X-VIVO basal complete containing 10 ng/mL human interleukin-4 (hIL-4) (Peprotech 130-093-924).

After successful monocyte to macrophage polarisation, the macrophages were detached by incubating with Accutase for 10 min at 37 °C, after which the macrophages were flushed with ice-cold PBS. Cells that were still attached to the plate were scraped with a P1000 pipette.

2.5 Flow cytometry analysis of hiPSC- and PBMC-derived monocytes and macrophages

To analyse hiPSC and PBMC-derived monocytes and macrophages, we created three flow cytometry panels:

- The monocyte characterisation panel: this flow cytometry panel was used for monocyte characterisation into classical, non-classical and intermediate monocytes based on CD14 and CD16 expression, as well as determination of monocyte maturity and inflammatory potential based on CCR2 and CX3CR1 expression (Table 4).
- The macrophage characterisation panel: this flow cytometry panel was used for macrophage characterisation into M0, M1 and M2 macrophages based on CD163, CD64, CD80 and CD206 expression (Table 5).
- The hiPSC-derived monocyte purity panel: this flow cytometry panel was used to determine monocyte purity in the hiPSC harvests based on CD14 and CD16 monocyte marker expression, cluster of differentiation (CD3) T-cell marker expression, cluster of differentiation (CD9) neutrophil marker expression and cluster of differentiation (CD19) B-cell marker expression (Table 6).

For the flow cytometry analysis of the monocytes and macrophages, cells were resuspended in 100 µL flow cytometry buffer (Ca^{+} and Mg^{2+} free PBS containing 5% heat inactivated FBS and 0.2% EDTA), after which a portion of cells from all conditions was transferred to the blank condition as a negative control. All conditions apart from the blank condition were stained with either the monocyte characterisation panel, macrophage characterisation panel or monocyte purity panel as displayed in the tables below for 30 min at 4 °C, after which the cells were washed with PBS and the viability staining was incubated for 30 min at 4 °C. The stained monocytes and macrophages were then centrifuged at 350 xG for 5 min, resuspended in 250 µL flow cytometry buffer and transferred to a 96-wells ultra-low attachment (ULA) plate and analysed on the Cytoflex (Beckman Coulter Inc, the Netherlands) using the CytExpert 2.2 software.

Table 4. Flow cytometry monocyte characterisation panel.

colour	Excitation (nm)	Filter	Marker	Clone	Isotype	Company	Catalogue number
AF647	645	660 BP 20	CD202b	33.1	Mouse IgG1	Biolegend	334210
AF700	645	725 BP 20	CD14	63D3	Mouse IgG1	Biolegend	367114
APC/Fire750	645	755 LP	CD11b	ICRF44	Mouse IgG1	Biolegend	301352
BV421	405	450 BP 50	CD115	9-4D2-1E4	Rat IgG1	Biolegend	347322
FITC	488	525 BP 40	CD31	WM59	Mouse IgG1	Biolegend	303104
PE	488	595 BP 30	CX3CR1	2A9-1	Mouse IgG1??	Biolegend	341604
PC7	488	755 LP	CD192 (CCR2)	K036C2	Mouse IgG1	Biolegend	357212
PerCP/Cy5.5	488	695 BP 30	CD16	3G8	Mouse IgG1	Biolegend	302028
Zombie yellow	405	550 BP 40	Viability			Biolegend	L34968

Table 5. Flow cytometry macrophage characterisation panel

Colour	Excitation (nm)	Marker	Clone	Isotype	Company	Catalogue number
BV785	405	CD206 (MMR)	15-2	Mouse IgG1	Biolegend	321141
PE	488	CD163	GHI/61	Mouse IgG1	Biolegend	333605
BV421	405	CD64	10.1	Mouse IgG1	Biolegend	305019
FITC	488	CD11B	ICRF44	Mouse IgG1	Biolegend	301329
APC	645	CD80	2D10	Mouse IgG1	Biolegend	305219
Zombie NIR	633	Viability			Biolegend	423105

Table 6. Flow cytometry hiPSC monocyte purity panel.

Colour	Excitation (nm)	Marker	Clone	Isotype	Company	Catalogue number
BV510	405	CD3	OKT-3	Mouse IgG1	Biolegend	317332
PE	488	CD9	# 209306	Mouse IgG2B	R&D systems	FAB1880P
PERCP 5.5	488	CD14	163D3	Mouse IgG1	Biolegend	367110
EFluor 450	405	CD19	eBio1D3	Rat / IgG2a, kappa	eBioscience	48-0193-82
BV785	405	CD16	3G8	Mouse IgG1	Biolegend	302046
Zombie NIR	633	Viability			Biolegend	423105

2.6 hiPSC-derived monocyte-EC interactions under flow

As a functional experiment, we analysed hiPSC-derived monocyte-EC interactions after hiPSC monocyte stimulation with TNF-α (Peprotech 300-01A) under flow using the IBIDI pump system. The day prior to the IBIDI experiment 2.4 x 10^5 hiPSC-ECs were resuspended in 150 µL iPSC-EC complete medium and attached to a µ-Slide (IBIDI 80186, Germany) for 2 hours at 37 °C. Afterwards the slides were connected to an IBIDI perfusion set (yellow and green, 50 cm, ID 1.6 mm; IBIDI 250210) which was filled with 10 mL iPSC-EC complete medium. The air bubbles within the tubing were removed by running the air bubble removal program for 30 min (IBIDI PumpControl software; Flow Parameters: pressure: 30.0 mbar, flow rate: 18.47 ml/min, unidirectional: 10.00 s and oscillating 0.50 s). The working program was then initiated (Flow parameters: pressure: 9.3 mbar, flow rate: 4.99 ml/min, shear stress: 3.00 dyn (pressure unit)/cm^2, shear rate: 300 1/s, unidirectional: 20.00 s and oscillating 0.50 s) and ran overnight.

The next day, hiPSC monocytes were harvested as described above. In total 5.0 x 10^5 to 2.0 x 10^6 of these monocytes, dependent on the monocyte harvest (equal number of monocytes within one experiment) were resuspended in X-VIVO basal complete medium and plated out in a 96-wells ULA plate. Half of these monocytes were stimulated with 10 ng/mL TNF-α for 4 hours. Simultaneously, the iPSC-EC complete medium in the IBIDI pump system was replaced with iPSC-EC starvation medium (Endothelial cell basal medium-2 containing 1% Pen/Strep and 0.5% FBS). After 4 hours, the TNF-α stimulated monocytes and control monocytes were flown over the hiPSC-ECs for 2 hours, after which the experiment was terminated and the slides fixated with 4% M/V paraformaldehyde (PFA) (Klinipath 4186, the Netherlands).

2.7 Monocyte adherence under flow: hiPSC endothelial cell and monocytes staining

To analyse monocyte adherence, ECs and monocytes were stained with CD31 and CD68, respectively. Cells were permeabilized with 0.1% Triton X-100/PBS (Sigma-Aldrich T9284_500mL, USA) for 10 min at RT after which the slides were blocked with 10% normal goat serum (NGS) (Vector Laboratories S1000, USA) in PBS for 60 min at RT. After 1 hour the primary antibodies CD31 polyclonal rabbit anti-human (Santa Cruz Technologies SC-1506, USA; 1:300) and CD68 monoclonal mouse anti-human (Invitrogen 14-0688-82; 1:300) in 1% PBSA (Bovine Serum Albumin Fraction V; Sigma-Aldrich 10735086001, Germany; in PBS) were incubated at 4 °C overnight. The next morning, secondary antibodies Goat anti-Mouse IgG (Alexa Fluor 488; 1:400 in 1% PBSA; Invitrogen A11001, USA) and Goat anti-Rabbit IgG (AlexaFluor 555; 1:400 in 1% PBSA; Invitrogen A21428) were incubated for 60 min at RT in the dark. Finally, the nuclei of the cells were stained by incubating Hoechst (Invitrogen H1399; 1:10 000 in PBS) for 3 min at RT in the dark. Analysis of the slides was performed on the OLYMPUS BX53 (DP71) at 10x magnification. During analysis, number of adherent monocytes were counted on 5 randomly selected points of the IBIDI slide. The mean of the number of adhered monocytes was then compared between control monocytes and monocytes activated with TNF-α.

3. Results

3.1 Hematopoietic differentiation of hiPSC-derived monocytes from three healthy donors

To investigate, if hiPSCs-derived monocytes and macrophages from three donors NP0 143-18, NP0 115-4H and NP0 144-41 phenotypically resembled PBMC-derived monocytes and macrophages as defined in Fig. 1, hiPSCs from these three donors were first differentiated into monocytes. Fig. 3A displays the different stages of the hiPSC to monocyte differentiation for all three cell lines. After four days of maturation, EBs were successfully created for all three donors and were equally mature based on structure and core density (Fig. 3A left). After ten days, successful outgrowth formation could be distinguished in all three cell lines, which closely resembled stromal like cells attached to the bottom of the well (Fig. 3A middle; scalebar 400 µm). From day 18 on, round and granulated cells (proofing definition 1 shown in Fig. 1) which phenotypically resembled monocytes were formed within the outgrowths (Fig. 3A right; scalebar 200 µm and column 4; scalebar 100 µm). These hiPSC-derived monocytes were harvested weekly for the duration of 5 weeks, with a mean harvest of 5.0 x 10^5 monocytes per well per week (Fig. 3B).

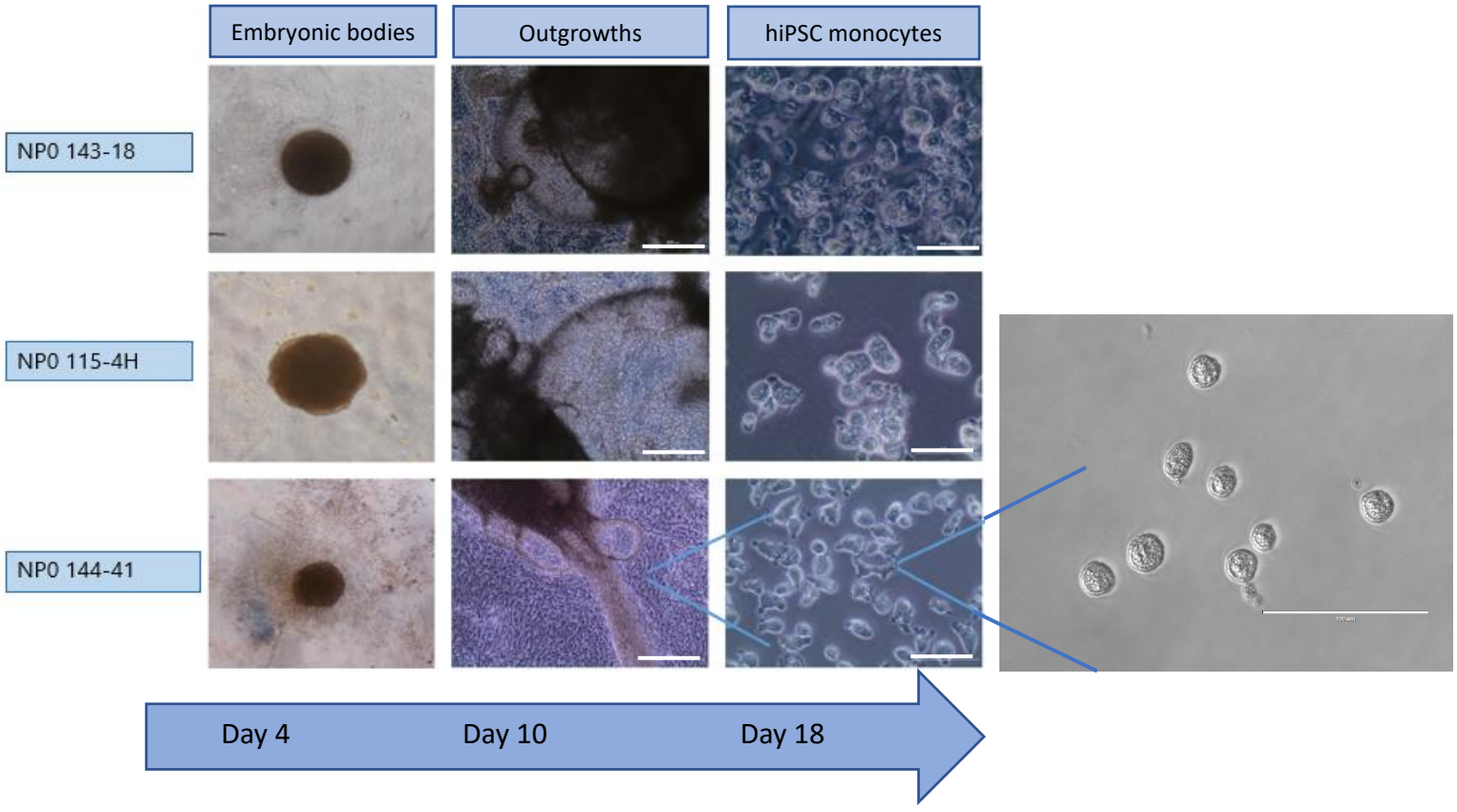

Figure 3A. hiPSC to monocyte differentiation of cell lines NP0 143-18, NP0 115-4H and NP0 144-41. *EBs were successfully generated for all 3 hiPSC donors (left). After EB maturation, they were transferred to gelatine coated 6-wells plates and formed outgrowths after approximately 10 days (middle; scalebar 400 µm). From day 18 onwards, outgrowths produced round granulated cells which phenotypically resembled monocytes (right; scalebar 200 µm and column 4; scalebar 100 µm).*

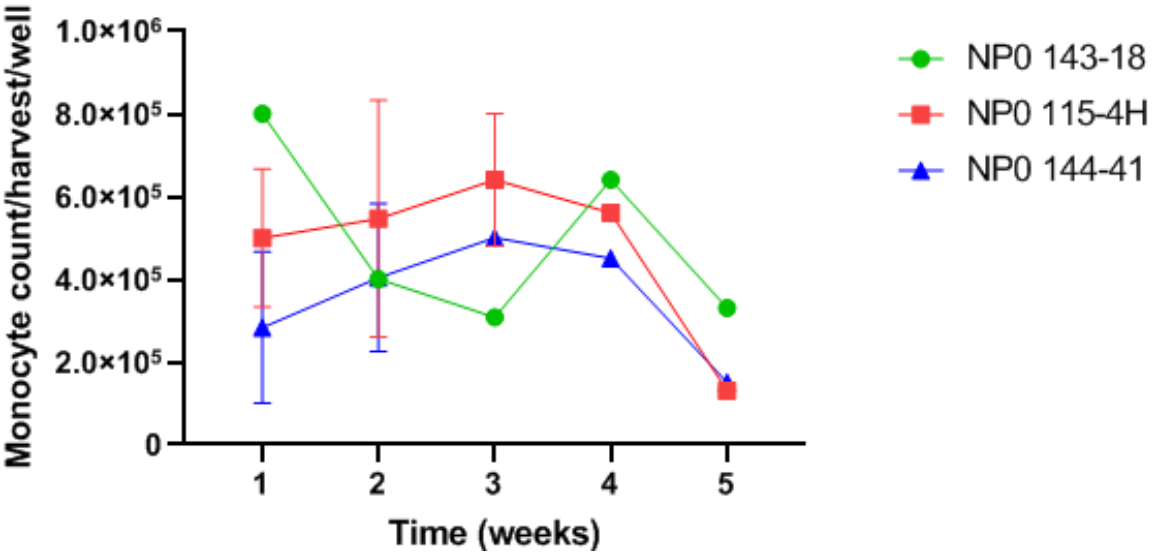

Figure 3B. hiPSC monocyte harvest per cell line per week. *hiPSC-derived monocyte counts per harvest per well are displayed, with monocyte counts of the 3 hiPSC donors on the Y-axis and harvest week on the X-axis. N=2 for cell lines NP0 144-41 and NP0 115-4H week 1-3.*

3.2 Characterisation of hiPSC-derived monocytes

The harvested monocytes were further characterised to prove production of viable monocytes, compare monocyte marker expression to blood-derived monocytes as defined in Fig 1 definition 2, and exclude production of other immune cells including T-cells, B-cells and neutrophils. For monocyte characterization, flow cytometry analysis was performed on monocyte markers CD14, CD16, CCR2 and CX3CR1 in week 1, 3 and 5 to analyse monocyte subsets and to prove consistent production of the same monocyte subsets (Fig. 4A), flow cytometry gating strategy is described in Supplementary Fig. 1. As Fig. 4A column 1 illustrates, most harvested monocytes were $CD14^{++}$ $CD16^{-}$ classical monocytes (about 60% of the viable monocyte population), except for NP0 143-18 and NP0 115-4H harvest 1. $CD14^{++}$ $CD16^{+}$ intermediate monocytes made-up a smaller percentage of the harvested monocytes (about 10%), while $CD14^{+}$ $CD16^{++}$ non-classical monocytes made up about 5% (Fig. 4A column 1). These results confirm that I produced hiPSC-derived monocytes, which could be classified into 3 distinct subsets based on CD14 CD16 expression as defined in Fig. 1 definition 2. Further monocyte characterization on monocyte maturity and inflammatory potential was performed using the CCR2 CX3CR1 scatterplots. Fig. 4A column 2 indicates that most of the harvested classical monocytes displayed an immature pro-inflammatory $CCR2^{+}$ phenotype consistent with hiPSC monocyte immaturity after harvesting, suggesting that harvested hiPSC monocytes resemble bone marrow monocytes in maturity as explained in the introduction. Intermediate monocytes, which are phenotypically in between classical and non-classical monocytes were positive for both CCR2 and CX3CR1 (Fig. 4A column 3), while a small increase in $CX3CR1^{+}$ cells could be seen in the non-classical monocyte subset, suggesting that the more mature anti-inflammatory monocytes were present in small quantities (about 3%) (Fig. 4A column 4).

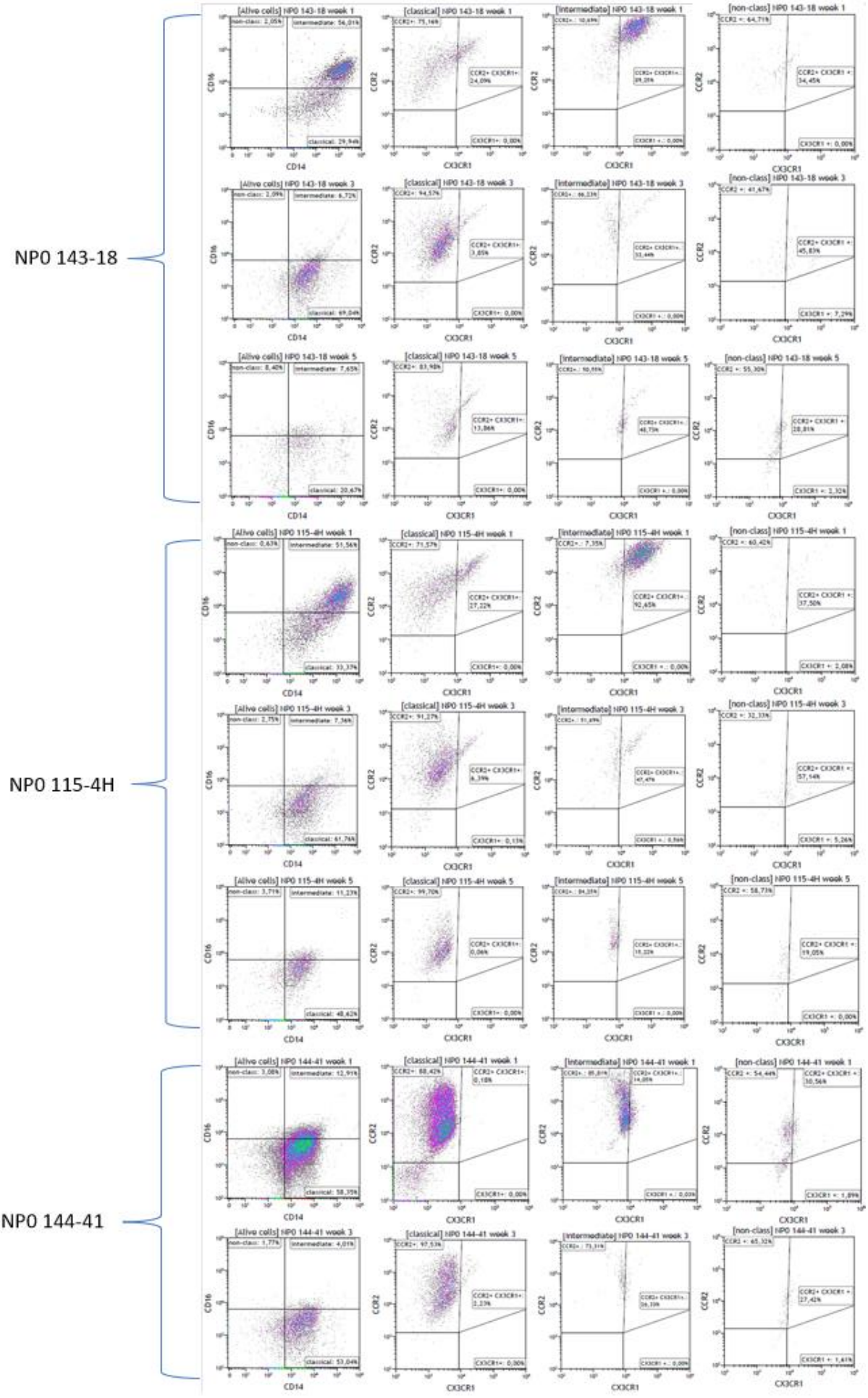

Figure 4A. Flow cytometry analysis of harvested hiPSC-derived monocytes. *hiPSC-derived monocytes harvested on weeks 1, 3 and 5 were analysed using flow cytometry on monocyte markers CD14 and CD16, and CCR2 and CX3CR1 to determine monocyte maturity and inflammatory potential. Most harvested monocytes were CD14^{++} CD16^{-} classical monocytes, with smaller non-classical and intermediate monocyte subsets (column 1). Further hiPSC-derived monocyte characterisation using the CCR2 CX3CR1 gating strategy illustrated that most of the harvested classical monocyte population displayed an immature pro-inflammatory CCR2^{+} phenotype(column 2). Intermediate monocytes were positive for both CCR2 and CX3CR1 (column 3), while a small increase in CX3CR1 positive cells could be distinguished in the non-classical monocyte subset (column 4).*

To investigate the potential of these hiPSC-derived monocytes to model human inflammation, the CD14, CD16, CCR2 and CX3CR1 flow cytometry analysis was repeated on PBMC-derived monocytes from MDD donors and compared to bone marrow monocytes analyses from literature (Patel, Zhang et al. 2017). The PBMC-derived monocytes showed comparable monocyte subset division, with a majority of $CCR2^{+}$ $CD14^{++}$ $CD16^{-}$ classical monocytes (17%), and smaller subsets of $CX3CR1^{+}$ $CD14^{+}$ $CD16^{++}$ non-classical monocytes (5%) and $CCR2^{+}$ $CD14^{++}$ $CD16^{+}$ intermediate monocytes (5%), while CD14 CD16 flow cytometry analysis of bone marrow biopsies and aspirates revealed that the bone marrow exclusively contains immature $CD14^{++}$ $CD16^{-}$ classical monocytes (Fig. 4B) (Patel, Zhang et al. 2017). Comparison of flow cytometry data revealed that the hiPSC-derived monocytes showed similarities to both bone marrow and PBMC-derived monocytes and are phenotypically in between these two cell types. Fig. 4C summarizes these flow cytometry data, displaying percentages of the classical-, non-classical- and intermediate monocyte populations per hiPSC donor per harvest with PMC-derived monocytes as control. To confirm monocyte purity, a flow cytometry analysis on the T-cell marker CD3 (Schuh, Berer et al. 2016), the neutrophil marker CD9 (Meeuwsen, de Vries et al. 2020) and the B-cell marker CD19 (Ferrara, Kolnik et al. 2018) was performed, while including monocyte markers CD14 and CD16 as positive control for monocytes. Fig. 4D illustrates a higher percentage of cells positive for monocyte markers CD14 and CD16 compared to blank, while T-cell marker CD3, neutrophil marker CD9 and B-cell marker CD19 are absent, confirming creation of hiPSC monocytes and no other immune cell types.

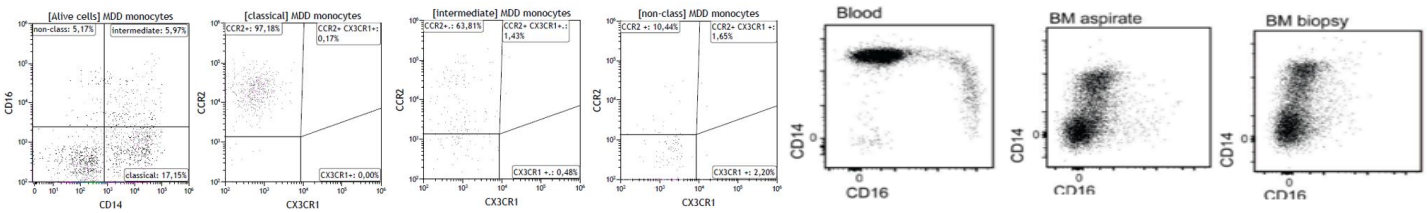

Figure 4B. Flow cytometry analysis of PBMC-derived monocytes and bone marrow monocytes. *To enable comparison of PBMC-derived, hiPSC-derived and bone marrow monocytes, a CD14, CD16, CCR2 and CX3CR1 flow cytometry analysis was performed on blood isolated PBMC-derived monocytes (scatterplot 1-4) and bone marrow monocytes (scatterplot 5-7). The bone marrow derived flow cytometry analysis was adapted from (Patel, Zhang et al. 2017).*

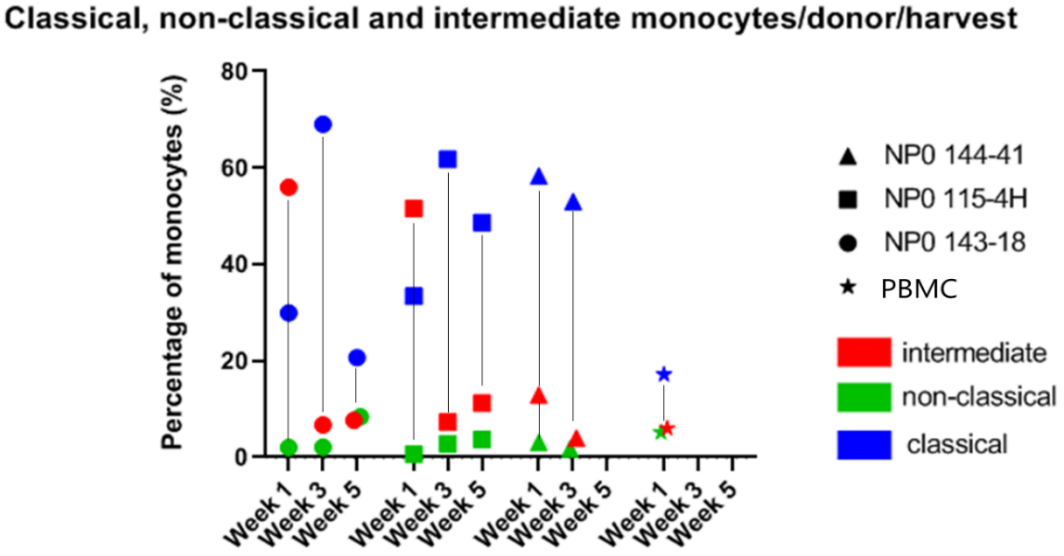

Figure 4C. Harvested hiPSC-derived monocyte subsets per donor per week. *Percentage of harvested monocyte subsets per donor per week is shown based on the CD14 CD16 flow cytometry scatterplots displayed in figure 4A and 4B, with the percentage of total monocytes on the y-axis, the harvested hiPSC-derived monocytes from all 3 donors per week on the X-axis and the different monocyte subsets in blue, red, and green.*

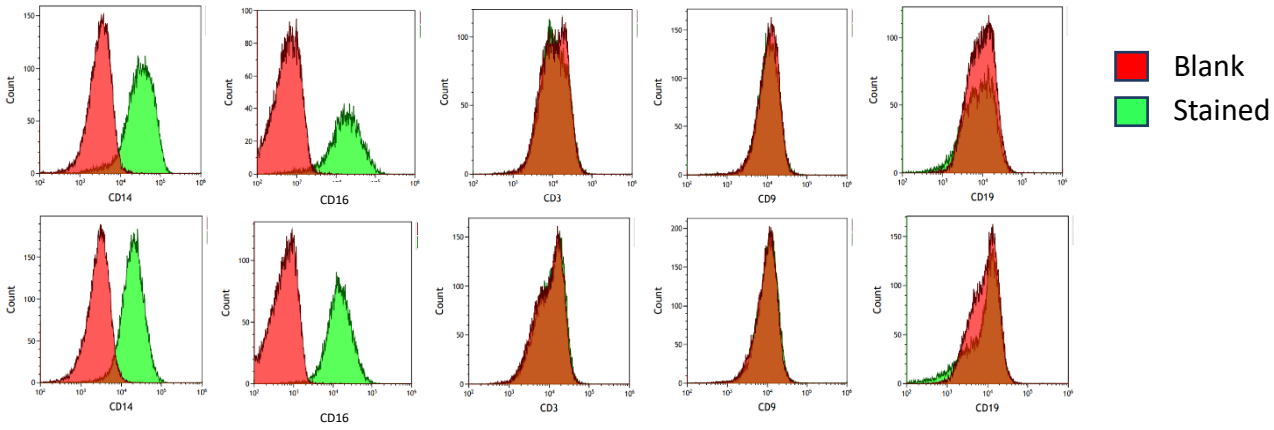

Figure 4D. Confirmation of harvested hiPSC-derived monocyte purity by flow cytometry. *To confirm purity of hiPSC-derived monocytes a flow cytometry analysis on harvested hiPSC monocytes was performed on the T-cell marker CD3, the neutrophil marker CD9 and the B-cell marker CD19. Monocyte markers CD14 and CD16 were used as control..*

3.3 Characterisation of hiPSC-derived M0, M1 and M2 macrophages

To further characterise the harvested hiPSC-derived monocytes, they were polarised towards macrophages (Italiani, Boraschi 2014). Fig. 5A shows the successful M0, M1 and M2 macrophage polarisation for all three donors (row 1, 2 and 3), confirming hiPSC-derived monocytes can differentiate towards macrophages as defined in Fig. 1 definition 4. To enable comparison, a schematic overview of human M0, M1 and M2 macrophage populations was adapted from (Wentzel, Petit et al. 2020) (row 4) showing similar phenotypic traits between hiPSC donors and the schematic control: clustered M1 macrophage populations and more stretched M2 macrophage phenotypes as defined in Fig. 1 definition 5.

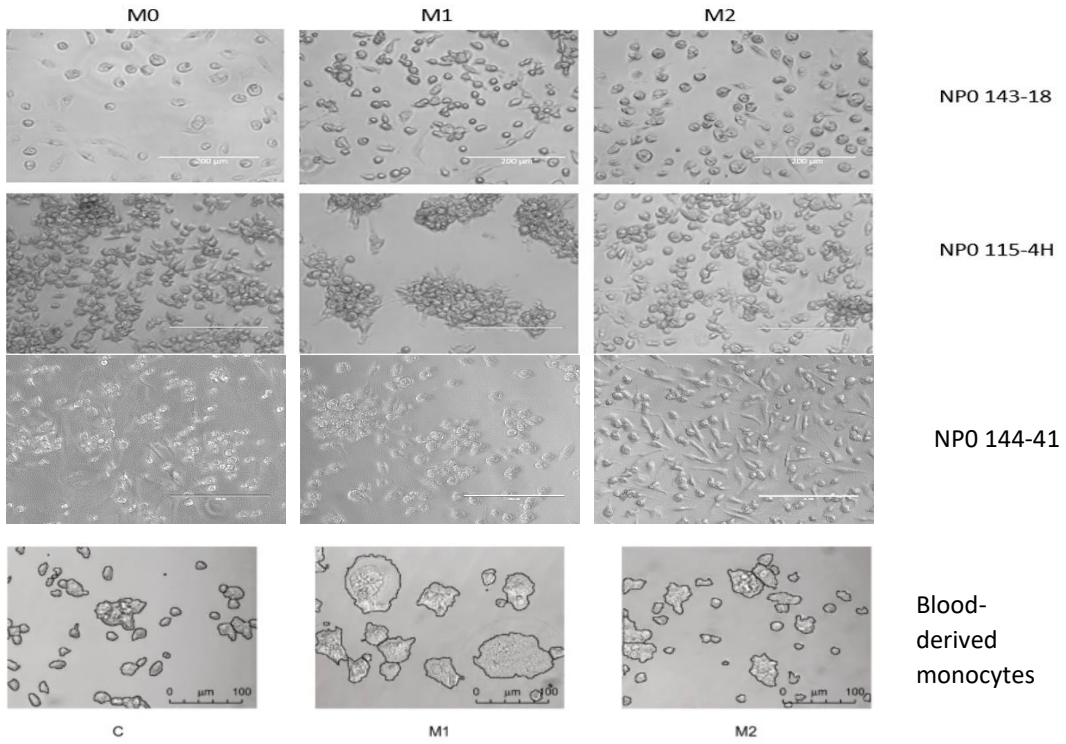

Figure 5A. hiPSC-derived monocyte to M0, M1 and M2 macrophage polarisation. *M0, M1 and M2 macrophages were successfully formed out of hiPSC-derived monocytes from all 3 donors (row 1-3). The bottom row of pictures displays a schematic overview of blood-derived M0, M1 and M2 macrophages adapted from Wentzel et al., 2020 to enable phenotype comparison of hiPSC-derived macrophages to human macrophage subsets.*

The polarised M0, M1 and M2 macrophages were then characterised using flow cytometry on general macrophage marker CD163, the M1 macrophage markers CD64 and the CD80 and M2 macrophage marker CD206 as defined in Fig. 1 definition 6 (Yao, Xu et al. 2019). Fig. 5B shows the scatterplots of this flow cytometry analysis for the M0, M1 and M2 macrophages of all three hiPSC donors and PBMC-derived macrophages. This same flow cytometry analysis is visualised in a histogram overlay (Fig. 5C) and in heatmaps that express percentage of positive cells per macrophage subtype per marker for all hiPSC donors and PBMC-derived macrophages (Supplementary Fig. 2). These 3 flow cytometry figures (Fig. 5B, Fig. 5C and Supplementary Fig. 2) illustrated an increase in CD163 marker expression in all 3 macrophage subsets of all hiPSC donors, confirming the ability of hiPSC-derived monocytes to polarise into phagocytotic macrophages (Fig. 1 definition 4). M1 macrophage markers CD80 and CD64 were increased in the M1 macrophage subsets, but not in the M0 and M2 macrophage subsets, illustrating the successful creation of M1 macrophages in all 3 hiPSC donors (Fig. 5B/5C). However, M2 macrophage marker CD206 was only increased in the M2 subset of hiPSC donor NP0 144-41, and showed equal expression in M0, M1 and M2 macrophages in the other 2 hiPSC donors (Fig. 5B/5C). These flow cytometry results suggest that while I am able to successfully create hiPSC-derived M1 macrophages, the creation of hiPSC-derived M2 macrophages is more difficult. This can be explained by the fact that I mainly harvest $CD14^{++}$ $CD16^{-}$ classical monocytes which polarise into pro-inflammatory M1 macrophages, while the number of $CD14^{+}$ $CD16^{++}$ non-classical monocytes, which polarise towards anti-inflammatory M2 macrophages is lower in the hiPSC monocyte harvests (Fig. 4A). I have now demonstrated that the classical, non-classical and intermediate hiPSC-derived monocytes are able to polarise towards their corresponding macrophage subset which are phenotypically distinct and closely resemble PBMC-derived macrophages. However, before these hiPSC-derived monocytes and macrophages can be used to model human inflammation, functional assessment (Fig. 1 definition 7 and 8) is required.

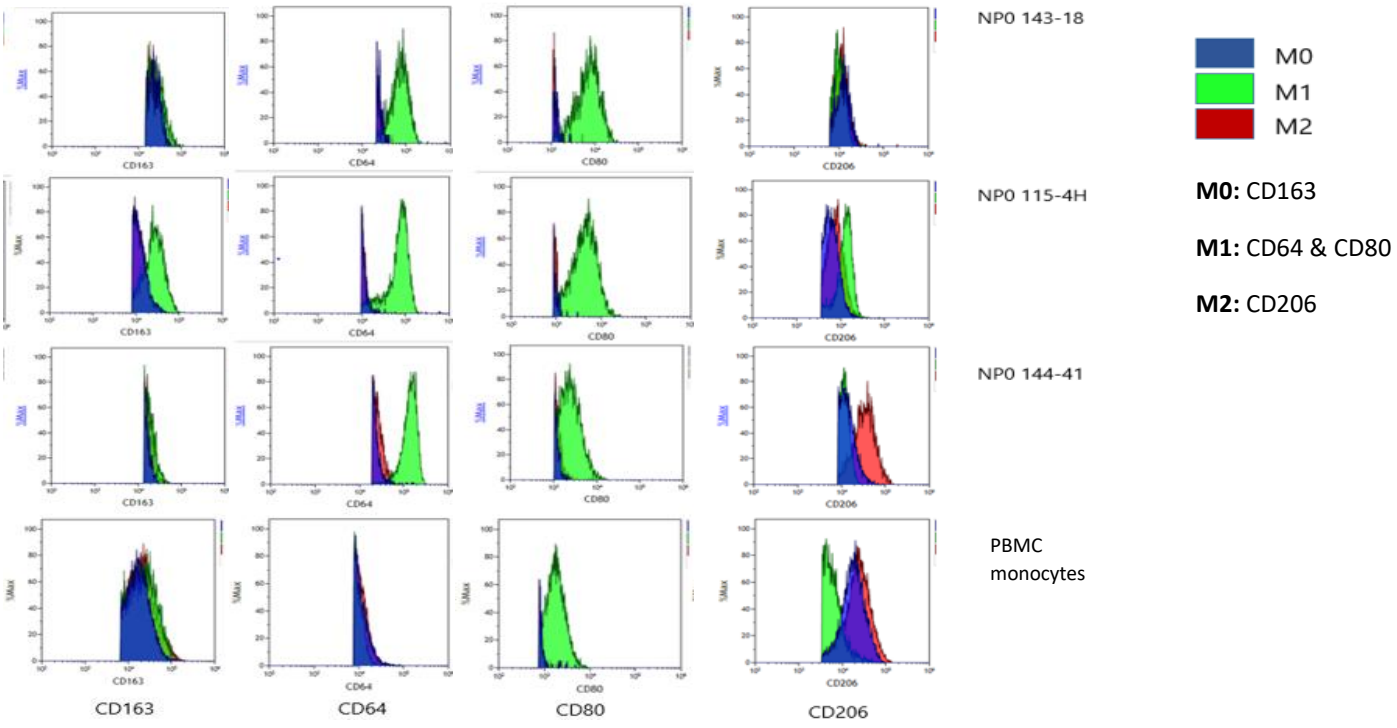

Figure 5C. Flow cytometry analysis of hiPSC and PBMC-derived M0, M1 and M2 macrophages – Histogram overlay. *A histogram overlay of general macrophage marker CD163, M1 macrophage markers CD80 and CD64 and M2 macrophage marker CD206, with the M0 macrophages (blue), M1 macrophages (green) and M2 (red) macrophage populations of each donor (row 1,2 and 3) and PBMC-derived macrophages (row 4) in the same histogram overlay plot to enable comparison.*

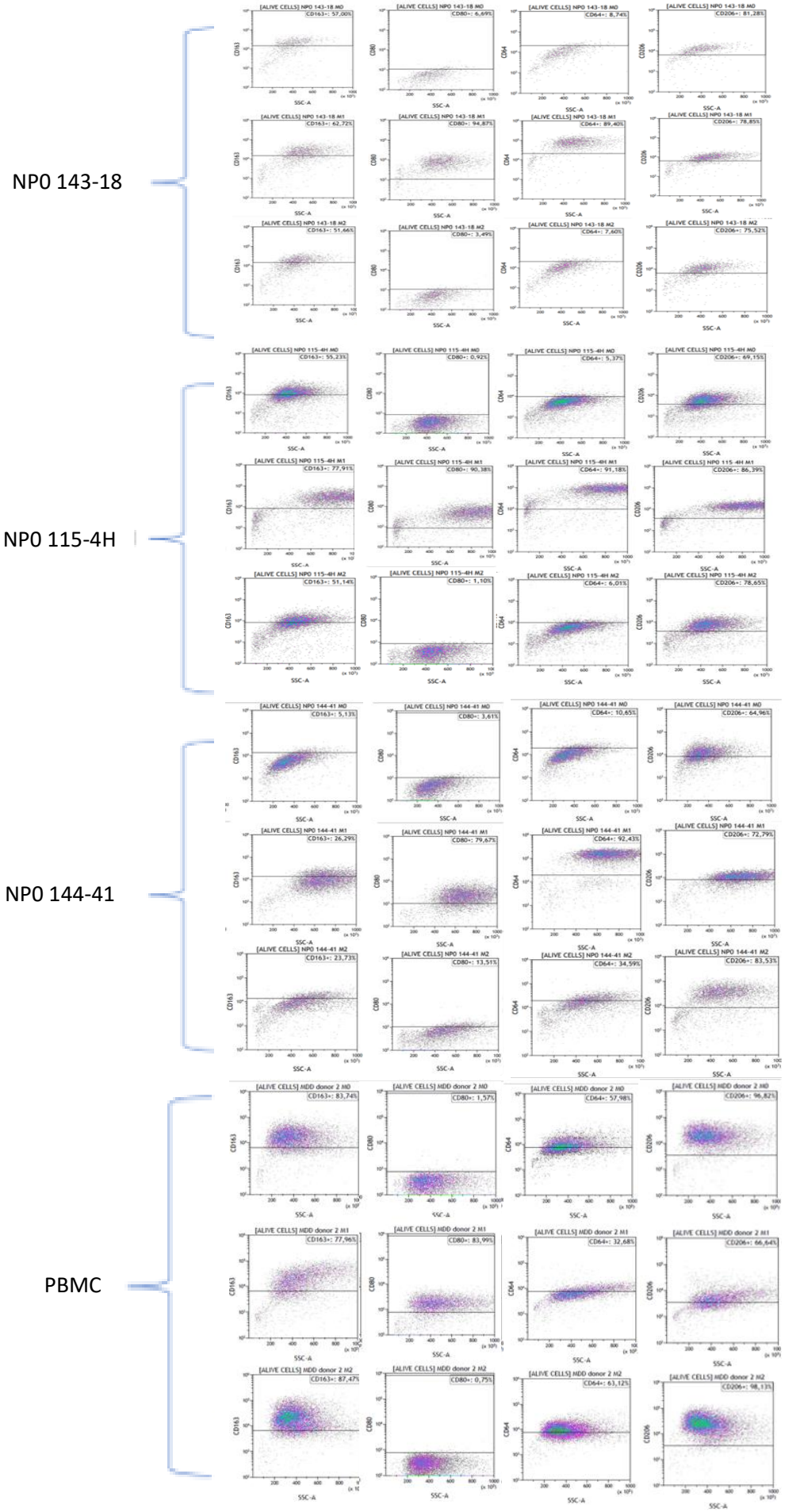

Figure 5B. Flow cytometry analysis of hiPSC- and PBMC- derived M0, M1 and M2 macrophages. *To characterise the hiPSC-derived M0, M1 and M2 macrophages, a flow cytometry analysis was performed on general macrophage marker CD163 (column 1), M1 macrophage markers CD80 and CD64 (column 2 and 3) and M2 macrophage marker CD206 (column 4). This figure shows the scatterplots of M0 (row 1 for each donor), M1 (row 2 for each donor) and M2 macrophages (row 3 for each donor) for the markers mentioned above for all 3 hiPSC donors, as well as PBMC-derived macrophages as a control.*

3.4 Functional characterisation of hiPSC-derived monocytes under flow

In addition to the phenotypical characterisation of the hiPSC-derived monocytes and macrophages, I performed a functional characterisation experiment. As defined in Fig. 1 definition 3, an important functional property of monocytes is adhesion to ECs and interaction with vasculature. Fig. 6A shows adherence of monocytes after monocyte adherence under flow using control or TNF-α stimulated hiPSC-derived monocytes and hiPSC-ECs from donors NP0 143-18 and NP0 115-4H. This figure illustrates increased monocyte adherence after monocyte activation with TNF-α for both NP0 143-18 EC conditions, with smaller increases in the NP0 115-4H EC conditions. Representative pictures of stained hiPSC-derived monocytes (top row), hiPSC-ECs (middle row) and cell nuclei (bottom row) are displayed in Fig. 6B. These results confirm that hiPSC-derived monocytes are functionally able to interact with the vasculature, and that iPSC monocyte-EC interactions increases after monocyte activation, which is an important functional property to include in models of human systemic inflammation.

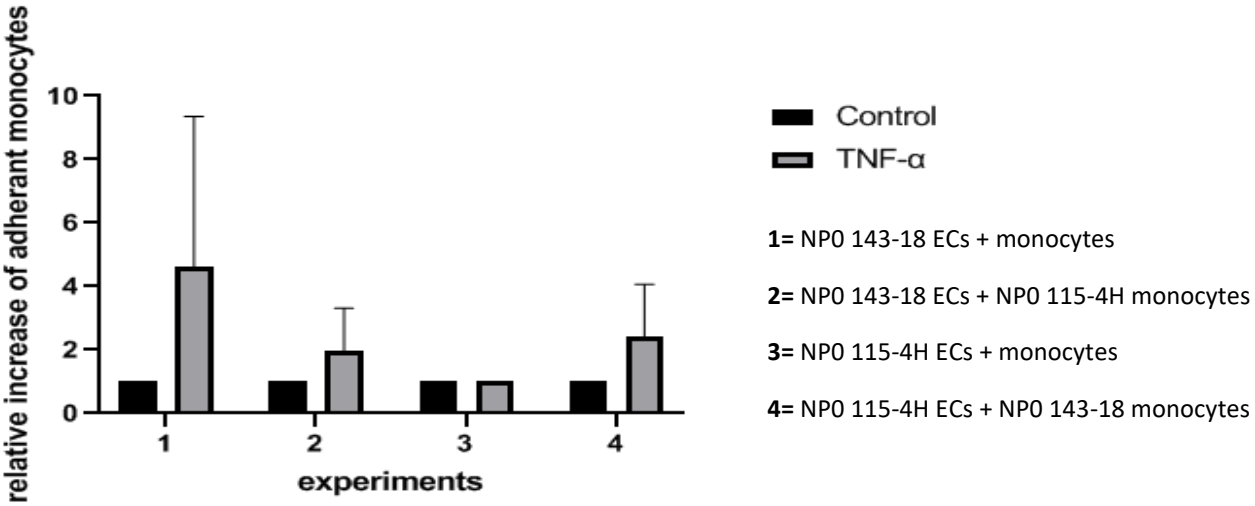

Figure 6A. IBIDI: hiPSC monocyte adherence under flow. *For the functional characterisation of hiPSC-derived monocytes, the harvested monocytes were stimulated with TNF-α and flown over hiPSC-ECs in the IBIDI flow system, with relative monocyte adherence of the Y-axis (control put on 1 for each separate experiment) and the different hiPSC monocyte and EC combinations on the X-axis. TNF-α activated monocytes showed increased monocyte adherence compared to control (approximately 2.5x increase in monocyte adherence).*

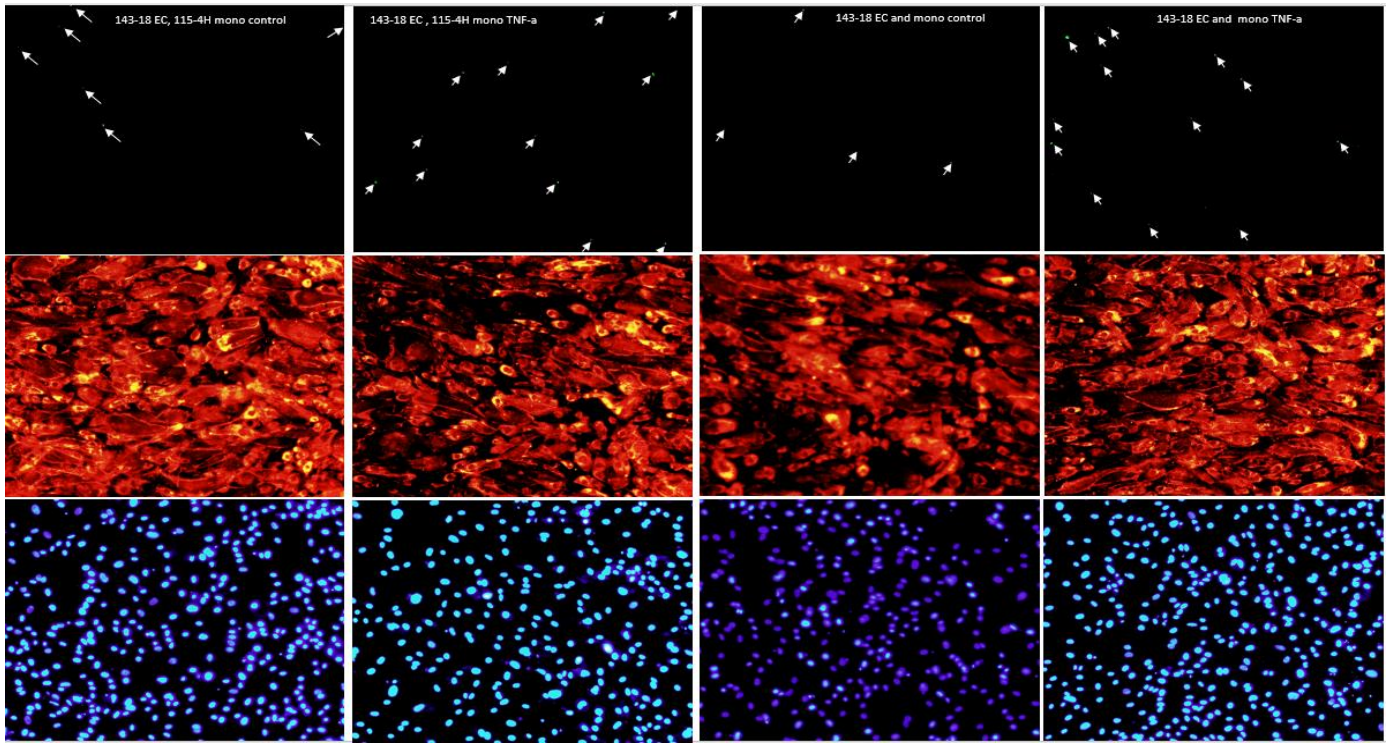

Figure 6B. IBIDI: hiPSC monocyte adherence under flow staining analysis. *Adherent hiPSC-derived monocytes (top row, individual adherent monocytes depicted with arrows), ECs (middle row) and their corresponding nuclei (bottom row) were stained. Corresponding with figure 4A, an increase in adhered hiPSC-derived monocytes can be observed after monocyte activation with TNF-α.*

4. Discussion

While the majority of CVDs are inflammation driven, monocytes and macrophages from the innate immune system are often not included in the *in vitro* models designed to study CVDs (Lippi, Stadiotti et al. 2020). Current research on the origin, development, and function of these innate immune cells utilise PBMC-derived monocytes and macrophages. However, these cells are hard to obtain in large quantities, are difficult to genetically modify, show batch-to-batch differences and are unable to produce tissue-resident macrophages, warranting a novel monocyte and macrophage cell source (Monkley, Krishnaswamy et al. 2020, van Wilgenburg, Browne et al. 2013).

I hypothesised that hiPSC-derived monocytes and macrophages are phenotypically and functionally similar to human PBMC-derived monocytes and macrophages and can in the future be used to model human inflammation in CVDs and vascular dysfunction. I illustrated the successful differentiation of three independent hiPSC cell lines into hiPSC-derived monocytes and macrophages and showed that these hiPSC-derived monocytes could be consistently harvested for all three cell lines, averaging approximately 5x10^5 cells per well of a 6-wells plate, which can easily be upscaled. I demonstrated that the harvested hiPSC-derived monocytes were round granulated cells, which could be divided into classical, non-classical and intermediate monocytes based on CD14 and CD16 expression. These monocytes were also able to interact with ECs and to polarise towards macrophages. hiPSC-derived macrophages were granulated cell types, which could be divided into M0, M1 and M2 macrophages based on CD163, CD64, CD80 and CD206 marker expression. These data provide substantial evidence that hiPSC-derived monocytes and macrophages closely resemble their PBMC-derived counterparts and are a promising cell type to model human inflammation in CVD *in vitro.* However, additional research to macrophage functionality and optimization of the differentiation protocol is required before I can confidently accept my hypothesis.

Additional experiments

Additional experiments to proof my hypothesis could include the determination of macrophage functionality, through internalisation of pathogens and cytokine secretion as defined in definition 7 and 8 of Fig. 1 (Kapellos, Bonaguro et al. 2019, Kratofil, Kubes et al. 2017). Future experiments should therefore compare hiPSC-derived macrophage phagocytotic ability to PBMC-derived macrophages, an example of which is the measurement of fluorescently labelled zymosan uptake previously illustrated by (Buchrieser, James et al. 2017). Additionally, pro-inflammatory cytokine (IL-6, TNF-α and IL-1β) and anti-inflammatory cytokine (IL-10) secretion of hiPSC-derived macrophages should be investigated in the different macrophage subsets and compared to PBMC-derived macrophages using e.g. ELISA, to illustrate pro-inflammatory M1 macrophage and anti-inflammatory M2 macrophage functionality, as previously illustrated (Cao, Yakala et al. 2019). Confirmation of hiPSC-derived macrophage functionality would provide additional evidence that hiPSC-derived monocytes and macrophages closely resemble their PBMC-derived counterparts and that they can be implemented in a CVD model to model human inflammation.

Limitations of generated monocyte types

One of the major limitations of the hiPSC to monocyte differentiation protocol lies within the hiPSC-monocyte subsets that are created and in the immaturity of this monocyte subset. As Fig. 4A and Fig. 4B illustrate, most of the hiPSC-derived monocytes belong to the immature $CD14^{++}$ $CD16^{-}$ classical monocyte subset, while little to no mature non-classical monocytes are produced similar to the human body, where classical monocytes make up approximately 85% of circulating monocytes (Patel, Zhang et al. 2017). The observation that I mainly created pro-inflammatory monocytes and their corresponding M1 macrophages suggest that hiPSC-derived monocytes and macrophages are

suitable to model pro-inflammatory processes in CVDs like chronic atherosclerosis, systemic inflammation and vascular dysfunction (Muhammad, Ayoub et al. 2021, Jaén, Val-Blasco et al. 2020). However, CVDs like chronic heart failure (HF), where anti-inflammatory processes facilitated by non-classical monocytes and their corresponding M2 macrophages cause and progress disease phenotype, cannot be modelled using the harvested hiPSC-derived monocytes and macrophages, due to low non-classical monocyte cell count and difficulty of M2 macrophage production (Adamo, Rocha-Resende et al. 2020, Tanai, Frantz 2015). This warrants tweaking of the differentiation protocol, to enable production of larger amounts of non-classical monocytes. Previous research has indicated that the bone marrow exclusively produces immature classical monocytes, which have a half-life of approximately 20 hours after entering the circulation and either transmigrate, die or give rise to intermediate and non-classical monocytes (Patel, Zhang et al. 2017, Yona, Kim et al. 2013). A logical thought would therefore be to remove the produced hiPSC-derived classical monocytes from their niche, plate them out and let them mature into non-classical monocytes. This is practically not feasible however, since hiPSC-monocyte plating on plastic can cause phenotype alterations and activation (Sauter, Yi et al. 2019). Additionally, research has elucidated that neurogenic locus notch homolog protein 2 (Notch 2) signalling, through Notch 2 activation with Notch ligand delta-like 1 (Dll1) produced by ECs, controls classical to non-classical monocyte conversion (Gamrekelashvili, Giagnorio et al. 2016). Future experiments should therefore include the co-culture of Dll1 during the hiPSC to monocyte differentiation, either after monocyte harvest or fully included within the differentiation protocol by supplementing MM differentiation medium with Dll1, in order to research hiPSC-derived non-classical monocyte production. Control over produced monocyte subsets would allow for customization of harvested classical, non-classical and intermediate monocytes to perfectly match your research question and specific CVDs or mechanisms you want to investigate.

Future perspectives

The next step would be to incorporate these hiPSC-derived monocytes and macrophages in advanced 3D models like cardiac organoids, that fully mimic the cardiac cell type composition, cardiac structure including extracellular matrix (ECM) and cardiac function (Seguret, Vermersch et al. 2021). Current cardiac organoid models usually comprise of CMs, fibroblasts and ECs and are able to recapitulate the complex 3D organization of the native human heart (Seguret, Vermersch et al. 2021, Lewis-Israeli, Wasserman et al. 2021). While CVDs like hypertrophic cardiomyopathy, restrictive cardiomyopathy and dilated cardiomyopathy have readily been modelled within these cardiac organoids, immune cells which promote and influence many other CVDs are not included (Seguret, Vermersch et al. 2021). Recent research has illustrated the use of antibody- based immunotherapy and cytokines within cardiac organoids to model inflammation-induced cardiac dysfunction and cardiac toxicity within these organoids, mimicking monocyte and macrophage function (Mills, Humphrey et al. 2021, Kumar, Thangavel et al. 2020). However, monocyte and macrophage phenotype and function is altered based on the signals provided by their local environment, displaying intricate crosstalk between monocytes and macrophages and their surrounding CMs, fibroblasts and ECs (Roberts, Lee et al. 2017, A-Gonzalez, Quintana et al. 2017). To accurately model monocyte and macrophage interactions with their environment, in order to research their contribution to CVD onset and progression within the human body, functional hiPSC-derived monocytes and macrophages should be included within these cardiac organoid models. These models can be customised by genetically modifying these hiPSC-derived monocytes and macrophages to precisely mimic CVDs genetics, enabling controlled and translatable research to CVD mechanisms and drug testing (Cui, Franz et al. 2021). Future research should therefore focus on the incorporation of these hiPSC-derived monocytes and macrophages in advanced 3D cardiac models, to

accurately mimic inflammation-induced CVD onset, progression, and pathophysiologic mechanisms, allowing for better understanding of these diseases and creating a novel platform for drug screening.

Conclusion

In conclusion, hiPSC-derived monocytes and macrophages phenotypically resemble their PBMC-derived counterparts and are a promising cell type to mimic human inflammation in CVDs *in vitro.* However, further functional characterisation of hiPSC-derived macrophages, as well as more control over produced monocyte subsets is required before these cells can be used to mimic human inflammation. therefore, I can partially accept my hypothesis, stating that sufficient evidence is provided to suggest that hiPSC-derived monocytes and macrophages are a suitable cell type to model pro-inflammatory CVDs and vascular dysfunction *in vitro.* However, for the modelling on anti-inflammatory processes within these CVDs, further tweaking of the protocol is required. In the future, these hiPSC-derived monocytes and macrophages should be included in complex 3D cardiac models to include tissue context and to research monocyte and macrophage contribution to inflammation driven CVDs and better understand disease mechanisms, enabling the creation of novel treatment options.

Supplementary figures

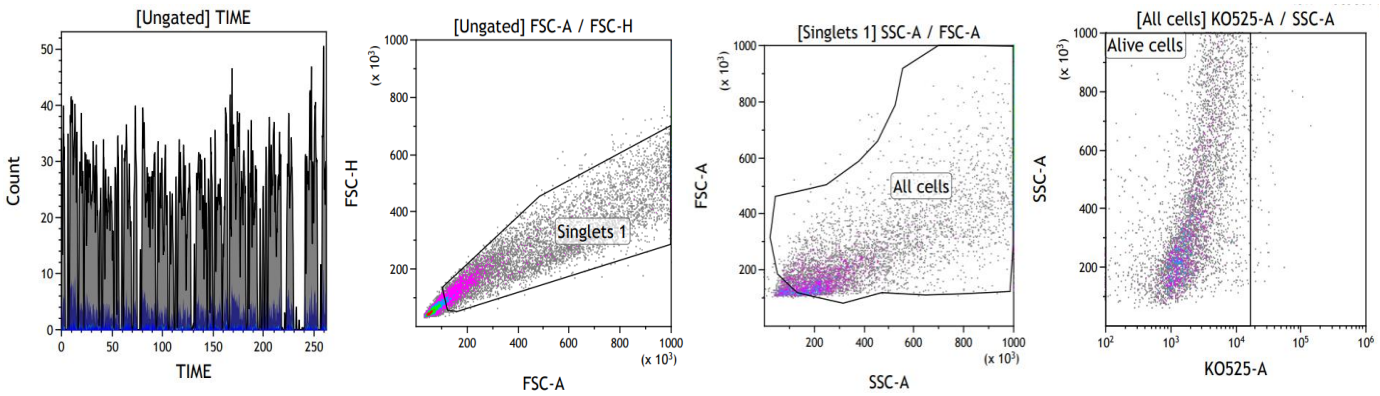

Supplementary figure 1. Flow cytometry analysis gating strategy. *Before every flow cytometry analysis, cells were gated for singlets to remove duplicates and triplicates from the analysis, debris was then removed by gating for all cells, after which the dead cells were excluded from the analysis using the viability dye.*

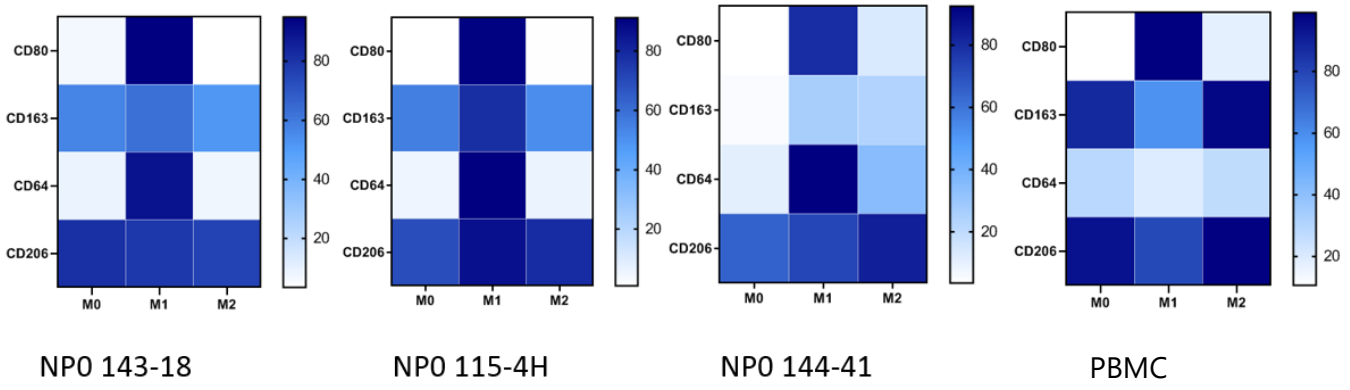

Supplementary Figure 2. Flow cytometry analysis of iPSC- and PBMC-derived M0, M1 and M2 macrophages – Heatmap percentage positive cells. *A heatmap overview with percentage positive cells of the flow cytometry data including general macrophage marker CD163, M1 macrophage markers CD80 and CD64 and M2 macrophage marker CD206 for macrophages from all three hiPSC donors and PBMC-derived macrophages as control.*

References

ADAMO, L., ROCHA-RESENDE, C., PRABHU, S.D. and MANN, D.L., 2020. Reappraising the role of inflammation in heart failure. *Nature reviews.Cardiology,* **17**(5), pp. 269-285.

A-GONZALEZ, N., QUINTANA, J.A., GARCÍA-SILVA, S., MAZARIEGOS, M., GONZÁLEZ DE LA ALEJA, A., NICOLÁS-ÁVILA, J.A., WALTER, W., ADROVER, J.M., CRAINICIUC, G., KUCHROO, V.K., ROTHLIN, C.V., PEINADO, H., CASTRILLO, A., RICOTE, M. and HIDALGO, A., 2017. Phagocytosis imprints heterogeneity in tissue-resident macrophages. *The Journal of experimental medicine,* **214**(5), pp. 1281-1296.

AL-RASHOUDI, R., MOIR, G., AL-HAJJAJ, M.S., AL-ALWAN, M.M., WILSON, H.M. and CRANE, I.J., 2019. Differential expression of CCR2 and CX(3)CR1 on CD16(+) monocyte subsets is associated with asthma severity. *Allergy, asthma, and clinical immunology : official journal of the Canadian Society of Allergy and Clinical Immunology,* **15**, pp. 64-5. eCollection 2019.

BUCHRIESER, J., JAMES, W. and MOORE, M.D., 2017. Human Induced Pluripotent Stem Cell-Derived Macrophages Share Ontogeny with MYB-Independent Tissue-Resident Macrophages. *Stem cell reports,* **8**(2), pp. 334-345.

CAO, X., YAKALA, G.K., VAN DEN HIL, F. E., COCHRANE, A., MUMMERY, C.L. and ORLOVA, V.V., 2019. Differentiation and Functional Comparison of Monocytes and Macrophages from hiPSCs with Peripheral Blood Derivatives. *Stem cell reports,* **12**(6), pp. 1282-1297.

CHOI, K.D., VODYANIK, M.A. and SLUKVIN, I.I., 2009. Generation of mature human myelomonocytic cells through expansion and differentiation of pluripotent stem cell-derived lin-CD34+CD43+CD45+ progenitors. *The Journal of clinical investigation,* **119**(9), pp. 2818-2829.

CUI, D., FRANZ, A., FILLON, S.A., JANNETTI, L., ISAMBERT, T., FUNDEL-CLEMENS, K., HUBER, H.J., VIOLLET, C., GHANEM, A., NIWA, A., WEIGLE, B. and PFLANZ, S., 2021. High-Yield Human Induced Pluripotent Stem Cell-Derived Monocytes and Macrophages Are Functionally Comparable With Primary Cells. *Frontiers in cell and developmental biology,* **9**, pp. 656867.

DOU, D.R., CALVANESE, V., SIERRA, M.I., NGUYEN, A.T., MINASIAN, A., SAARIKOSKI, P., SASIDHARAN, R., RAMIREZ, C.M., ZACK, J.A., CROOKS, G.M., GALIC, Z. and MIKKOLA, H.K., 2016. Medial HOXA genes demarcate haematopoietic stem cell fate during human development. *Nature cell biology,* **18**(6), pp. 595-606.

FERRARA, F., KOLNIK, M., D'ANGELO, S., ERASMUS, F.M., VORHOLT, D. and BRADBURY, A.R.M., 2018. Rapid purification of billions of circulating CD19+ B cells directly from leukophoresis samples. *New biotechnology,* **46**, pp. 14-21.

GAMREKELASHVILI, J., GIAGNORIO, R., JUSSOFIE, J., SOEHNLEIN, O., DUCHENE, J., BRISEÑO, C.G., RAMASAMY, S.K., KRISHNASAMY, K., LIMBOURG, A., KAPANADZE, T., ISHIFUNE, C., HINKEL, R., RADTKE, F., STROBL, L.J., ZIMBER-STROBL, U., NAPP, L.C., BAUERSACHS, J., HALLER, H., YASUTOMO, K., KUPATT, C., MURPHY, K.M., ADAMS, R.H., WEBER, C. and LIMBOURG, F.P., 2016. Regulation of monocyte cell fate by blood vessels mediated by Notch signalling. *Nature communications,* **7**, pp. 12597.

GINHOUX, F. and JUNG, S., 2014. Monocytes and macrophages: developmental pathways and tissue homeostasis. *Nature reviews.Immunology,* **14**(6), pp. 392-404.

GORDON, S. and TAYLOR, P.R., 2005. Monocyte and macrophage heterogeneity. *Nature reviews.Immunology,* **5**(12), pp. 953-964.

HAPPLE, C., LACHMANN, N., ACKERMANN, M., MIRENSKA, A., GÖHRING, G., THOMAY, K., MUCCI, A., HETZEL, M., GLOMB, T., SUZUKI, T., CHALK, C., GLAGE, S., DITTRICH-BREIHOLZ, O., TRAPNELL, B., MORITZ, T. and HANSEN, G., 2018. Pulmonary Transplantation of Human Induced Pluripotent Stem Cell-derived Macrophages Ameliorates Pulmonary Alveolar Proteinosis. *American journal of respiratory and critical care medicine,* **198**(3), pp. 350-360.

ITALIANI, P. and BORASCHI, D., 2014. From Monocytes to M1/M2 Macrophages: Phenotypical vs. Functional Differentiation. *Frontiers in immunology,* **5**, pp. 514.

JAÉN, R.I., VAL-BLASCO, A., PRIETO, P., GIL-FERNÁNDEZ, M., SMANI, T., LÓPEZ-SENDÓN, J.L., DELGADO, C., BOSCÁ, L. and FERNÁNDEZ-VELASCO, M., 2020. Innate Immune Receptors, Key Actors in Cardiovascular Diseases. *JACC.Basic to translational science,* **5**(7), pp. 735-749.

KAPELLOS, T.S., BONAGURO, L., GEMÜND, I., REUSCH, N., SAGLAM, A., HINKLEY, E.R. and SCHULTZE, J.L., 2019. Human Monocyte Subsets and Phenotypes in Major Chronic Inflammatory Diseases. *Frontiers in immunology,* **10**, pp. 2035.

KARLSSON, K.R., COWLEY, S., MARTINEZ, F.O., SHAW, M., MINGER, S.L. and JAMES, W., 2008. Homogeneous monocytes and macrophages from human embryonic stem cells following coculture-free differentiation in M-CSF and IL-3. *Experimental hematology,* **36**(9), pp. 1167-1175.

KRATOFIL, R.M., KUBES, P. and DENISET, J.F., 2017. Monocyte Conversion During Inflammation and Injury. *Arteriosclerosis, Thrombosis, and Vascular Biology,* **37**(1), pp. 35-42.

KUMAR, M., THANGAVEL, C., BECKER, R.C. and SADAYAPPAN, S., 2020. Monoclonal Antibody-Based Immunotherapy and Its Role in the Development of Cardiac Toxicity. *Cancers,* **13**(1), pp. 86. doi: 10.3390/cancers13010086.

LANG, J., CHENG, Y., ROLFE, A., HAMMACK, C., VERA, D., KYLE, K., WANG, J., MEISSNER, T.B., REN, Y., COWAN, C. and TANG, H., 2018. An hPSC-Derived Tissue-Resident Macrophage Model Reveals Differential Responses of Macrophages to ZIKV and DENV Infection. *Stem cell reports,* **11**(2), pp. 348-362.

LEE, C.Z.W., KOZAKI, T. and GINHOUX, F., 2018. Studying tissue macrophages in vitro: are iPSC-derived cells the answer? *Nature reviews.Immunology,* **18**(11), pp. 716-725.

LEONG, D.P., JOSEPH, P.G., MCKEE, M., ANAND, S.S., TEO, K.K., SCHWALM, J.D. and YUSUF, S., 2017. Reducing the Global Burden of Cardiovascular Disease, Part 2: Prevention and Treatment of Cardiovascular Disease. *Circulation research,* **121**(6), pp. 695-710.

LEWIS-ISRAELI, Y.R., WASSERMAN, A.H. and AGUIRRE, A., 2021. Heart Organoids and Engineered Heart Tissues: Novel Tools for Modeling Human Cardiac Biology and Disease. *Biomolecules,* **11**(9), pp. 1277. doi: 10.3390/biom11091277.

LICHANSKA, A.M., BROWNE, C.M., HENKEL, G.W., MURPHY, K.M., OSTROWSKI, M.C., MCKERCHER, S.R., MAKI, R.A. and HUME, D.A., 1999. Differentiation of the mononuclear phagocyte system during mouse embryogenesis: the role of transcription factor PU.1. *Blood,* **94**(1), pp. 127-138.

LIPPI, M., STADIOTTI, I., POMPILIO, G. and SOMMARIVA, E., 2020. Human Cell Modeling for Cardiovascular Diseases. *International journal of molecular sciences,* **21**(17), pp. 6388. doi: 10.3390/ijms21176388.

MANTOVANI, A., SICA, A., SOZZANI, S., ALLAVENA, P., VECCHI, A. and LOCATI, M., 2004. The chemokine system in diverse forms of macrophage activation and polarization. *Trends in immunology,* **25**(12), pp. 677-686.

MEEUWSEN, J.A.L., DE VRIES, J., ZOET, G.A., FRANX, A., FAUSER, B. C. J. M., MAAS, A. H. E. M., VELTHUIS, B.K., APPELMAN, Y.E., VISSEREN, F.L., PASTERKAMP, G., HOEFER, I.E., VAN RIJN, B.B., DEN RUIJTER, H.M. and DE JAGER, S. C. A., 2020. Circulating Neutrophils Do Not Predict Subclinical Coronary Artery Disease in Women with Former Preeclampsia. *Cells,* **9**(2), pp. 468. doi: 10.3390/cells9020468.

MILLS, R.J., HUMPHREY, S.J., FORTUNA, P.R.J., LOR, M., FOSTER, S.R., QUAIFE-RYAN, G.A., JOHNSTON, R.L., DUMENIL, T., BISHOP, C., RUDRARAJU, R., RAWLE, D.J., LE, T., ZHAO, W., LEE, L., MACKENZIE-KLUDAS, C., MEHDIABADI, N.R., HALLIDAY, C., GILHAM, D., FU, L., NICHOLLS, S.J., JOHANSSON, J., SWEENEY, M., WONG, N.C.W., KULIKOWSKI, E., SOKOLOWSKI, K.A., TSE, B.W.C., DEVILÉE, L., VOGES, H.K., REYNOLDS, L.T., KRUMEICH, S., MATHIESON, E., ABU-BONSRAH, D., KARAVENDZAS, K., GRIFFEN, B., TITMARSH, D., ELLIOTT, D.A., MCMAHON, J., SUHRBIER, A., SUBBARAO, K., PORRELLO, E.R., SMYTH, M.J., ENGWERDA, C.R., MACDONALD, K.P.A., BALD, T., JAMES, D.E. and HUDSON, J.E., 2021. BET inhibition blocks inflammation-induced cardiac dysfunction and SARS-CoV-2 infection. *Cell,* **184**(8), pp. 2167-2182.e22.

MONKLEY, S., KRISHNASWAMY, J.K., GÖRANSSON, M., CLAUSEN, M., MEULLER, J., THÖRN, K., HICKS, R., DELANEY, S. and STJERNBORG, L., 2020. Optimised generation of iPSC-derived macrophages and dendritic cells that are functionally and transcriptionally similar to their primary counterparts. *PloS one,* **15**(12), pp. e0243807.

MUHAMMAD, K., AYOUB, M.A. and IRATNI, R., 2021. Vascular Inflammation in Cardiovascular Disease: Is Immune System Protective or Bystander? *Current pharmaceutical design,* **27**(18), pp. 2141-2150.

NUGRAHA, B., BUONO, M.F., VON BOEHMER, L., HOERSTRUP, S.P. and EMMERT, M.Y., 2019. Human Cardiac Organoids for Disease Modeling. *Clinical pharmacology and therapeutics,* **105**(1), pp. 79-85.

PARISI, L., GINI, E., BACI, D., TREMOLATI, M., FANULI, M., BASSANI, B., FARRONATO, G., BRUNO, A. and MORTARA, L., 2018. Macrophage Polarization in Chronic Inflammatory Diseases: Killers or Builders? *Journal of immunology research,* **2018**, pp. 8917804.

PATEL, A.A., ZHANG, Y., FULLERTON, J.N., BOELEN, L., RONGVAUX, A., MAINI, A.A., BIGLEY, V., FLAVELL, R.A., GILROY, D.W., ASQUITH, B., MACALLAN, D. and YONA, S., 2017. The fate and lifespan of human monocyte subsets in steady state and systemic inflammation. *The Journal of experimental medicine,* **214**(7), pp. 1913-1923.

ROBERTS, A.W., LEE, B.L., DEGUINE, J., JOHN, S., SHLOMCHIK, M.J. and BARTON, G.M., 2017. Tissue-Resident Macrophages Are Locally Programmed for Silent Clearance of Apoptotic Cells. *Immunity,* **47**(5), pp. 913-927.e6.

SAUTER, A., YI, D.H., LI, Y., ROERSMA, S. and APPEL, S., 2019. The Culture Dish Surface Influences the Phenotype and Cytokine Production of Human Monocyte-Derived Dendritic Cells. *Frontiers in immunology,* **10**, pp. 2352.

SCHUH, E., BERER, K., MULAZZANI, M., FEIL, K., MEINL, I., LAHM, H., KRANE, M., LANGE, R., PFANNES, K., SUBKLEWE, M., GÜRKOV, R., BRADL, M., HOHLFELD, R., KÜMPFEL, T., MEINL, E. and KRUMBHOLZ, M., 2016. Features of Human CD3+CD20+ T Cells. *Journal of immunology (Baltimore, Md.: 1950),* **197**(4), pp. 1111-1117.

SEGURET, M., VERMERSCH, E., JOUVE, C. and HULOT, J.S., 2021. Cardiac Organoids to Model and Heal Heart Failure and Cardiomyopathies. *Biomedicines,* **9**(5), pp. 563. doi: 10.3390/biomedicines9050563.

TANAI, E. and FRANTZ, S., 2015. Pathophysiology of Heart Failure. *Comprehensive Physiology,* **6**(1), pp. 187-214.

VAN WILGENBURG, B., BROWNE, C., VOWLES, J. and COWLEY, S.A., 2013. Efficient, long term production of monocyte-derived macrophages from human pluripotent stem cells under partly-defined and fully-defined conditions. *PloS one,* **8**(8), pp. e71098.

VIRANI, S.S., ALONSO, A., BENJAMIN, E.J., BITTENCOURT, M.S., CALLAWAY, C.W., CARSON, A.P., CHAMBERLAIN, A.M., CHANG, A.R., CHENG, S., DELLING, F.N., DJOUSSE, L., ELKIND, M.S.V., FERGUSON, J.F., FORNAGE, M., KHAN, S.S., KISSELA, B.M., KNUTSON, K.L., KWAN, T.W., LACKLAND, D.T., LEWIS, T.T., LICHTMAN, J.H., LONGENECKER, C.T., LOOP, M.S., LUTSEY, P.L., MARTIN, S.S., MATSUSHITA, K., MORAN, A.E., MUSSOLINO, M.E., PERAK, A.M., ROSAMOND, W.D., ROTH, G.A., SAMPSON, U.K.A., SATOU, G.M., SCHROEDER, E.B., SHAH, S.H., SHAY, C.M., SPARTANO, N.L., STOKES, A., TIRSCHWELL, D.L., VANWAGNER, L.B., TSAO, C.W. and AMERICAN HEART ASSOCIATION COUNCIL ON EPIDEMIOLOGY AND PREVENTION STATISTICS COMMITTEE AND STROKE STATISTICS SUBCOMMITTEE, 2020. Heart Disease and Stroke Statistics-2020 Update: A Report From the American Heart Association. *Circulation,* **141**(9), pp. e139-e596.

WENTZEL, A.S., PETIT, J., VAN VEEN, W.G., FINK, I.R., SCHEER, M.H., PIAZZON, M.C., FORLENZA, M., SPAINK, H.P. and WIEGERTJES, G.F., 2020. Transcriptome sequencing supports a conservation of macrophage polarization in fish. *Scientific reports,* **10**(1), pp. 13470-y.

WILLIAMS, J.W., HUANG, L.H. and RANDOLPH, G.J., 2019. Cytokine Circuits in Cardiovascular Disease. *Immunity,* **50**(4), pp. 941-954.

WONG, K.L., TAI, J.J., WONG, W.C., HAN, H., SEM, X., YEAP, W.H., KOURILSKY, P. and WONG, S.C., 2011. Gene expression profiling reveals the defining features of the classical, intermediate, and nonclassical human monocyte subsets. *Blood,* **118**(5), pp. 16.

YANAGIMACHI, M.D., NIWA, A., TANAKA, T., HONDA-OZAKI, F., NISHIMOTO, S., MURATA, Y., YASUMI, T., ITO, J., TOMIDA, S., OSHIMA, K., ASAKA, I., GOTO, H., HEIKE, T., NAKAHATA, T. and SAITO, M.K., 2013. Robust and highly-efficient differentiation of functional monocytic cells from human pluripotent stem cells under serum- and feeder cell-free conditions. *PloS one,* **8**(4), pp. e59243.

YAO, Y., XU, X.H. and JIN, L., 2019. Macrophage Polarization in Physiological and Pathological Pregnancy. *Frontiers in immunology,* **10**, pp. 792.

YONA, S., KIM, K.W., WOLF, Y., MILDNER, A., VAROL, D., BREKER, M., STRAUSS-AYALI, D., VIUKOV, S., GUILLIAMS, M., MISHARIN, A., HUME, D.A., PERLMAN, H., MALISSEN, B., ZELZER, E. and JUNG, S., 2013. Fate mapping reveals origins and dynamics of monocytes and tissue macrophages under homeostasis. *Immunity,* **38**(1), pp. 79-91.